



1   **Rapid environmental responses to climate-induced hydrographic changes in**  
2   **the Baltic Sea entrance**

3   LAURIE M. CHARRIEAU<sup>1</sup>, KARL LJUNG<sup>1</sup>, FREDERIK SCHENK<sup>2</sup>, UTE DAEWEL<sup>3</sup>, EMMA  
4   KRITZBERG<sup>4</sup> and HELENA L. FILIPSSON<sup>\*1</sup>

5   <sup>1</sup>Department of Geology, Lund University, Sweden

6   <sup>2</sup>Bolin Centre for Climate Research and Department of Geological Sciences, Stockholm University, Sweden

7   <sup>3</sup>Department of System Analysis and Modelling, Centre for Materials and Coastal Research, Geesthacht,  
8   Germany

9   <sup>4</sup>Department of Biology, Lund University, Sweden

10   \*Corresponding author (address: Sölvegatan 12, SE-223 62; e-mail: [helena.filipsson@geol.lu.se](mailto:helena.filipsson@geol.lu.se))

11   Key-words: benthic foraminiferal; NAO index; environmental reconstruction; Anthropocene;  
12   Öresund

13   Abstract

14   The Öresund (the Sound), which is a part of the Danish straits, is linking the marine North Sea  
15   and the brackish Baltic Sea. It is a transition zone where ecosystems are subjected to large  
16   gradients in terms of salinity, temperature, carbonate chemistry, and dissolved oxygen  
17   concentration. In addition to the highly variable environmental conditions, the area is responding  
18   to anthropogenic disturbances in e.g. nutrient loading, temperature, and pH. We have  
19   reconstructed environmental changes in the Öresund during the last c. 200 years, and especially  
20   dissolved oxygen concentration, salinity, organic matter content, and pollution levels, using  
21   benthic foraminifera and sediment geochemistry. Five zones with characteristic foraminiferal  
22   assemblages were identified, each reflecting the environmental conditions for respective period.



23 The largest changes occurred ~1950, when the foraminiferal assemblage shifted from a low  
24 diversity fauna, dominated by the species *Stainforthia fusiformis* to higher diversity and  
25 abundance, and dominance of the *Elphidium* group. Concurrently, the grain-size distribution  
26 shifted from clayey — to more sandy sediment. To explore the causes for the environmental  
27 changes, we used time-series of reconstructed wind conditions coupled with large-scale climate  
28 variations as recorded by the NAO index, as well as the ECOSMO II model of currents in the  
29 Öresund area. The results indicate increased changes in the water circulation towards stronger  
30 currents in the area since the 1950's. The foraminiferal fauna responded quickly (< 10 years) to  
31 the environmental changes. Notably, when the wind conditions, and thereby the current system,  
32 returned in the 1980's to the previous pattern, the foraminiferal species assemblage did not  
33 rebound, but the foraminiferal faunas rather displayed a new equilibrium state.

34 1 – Introduction

35 The Öresund (the Sound) is one part of the Danish straits between Sweden and Denmark.  
36 Together with the Great — and Little Belt, they link the open-ocean waters of the North Sea and  
37 the brackish waters of the Baltic Sea. The confluence of the water masses creates a north-south  
38 gradient as well as a strong vertical stratification of the water in terms of salinity, carbonate  
39 chemistry and dissolved oxygen concentration ( $[O_2]$ ) (Leppäranta and Myrberg 2009). The depth  
40 of the halocline mainly depends of the outflows from the Baltic Sea; a strong thermocline  
41 develops during spring and summer, which further strengthens the vertical stratification. Thus,  
42 the ecosystems in the Öresund are exposed — and adapted — to a unique transitional  
43 environment. The region is also characterized by intense human activities, with 4 million people  
44 living in the vicinity of the Öresund and 85 million people living in the catchment area of the  
45 Baltic Sea. Discharge from agriculture, industry, and urban areas on both the Swedish and



46 Danish sides of the strait, and the considerable impact of marine traffic – the strait is one of the  
47 busiest waterways in the world – generate pollution and eutrophication of the water (HELCOM  
48 2009; ICES 2010). Since the 1980's, the implementation of efficient wastewater treatment and  
49 measures in agriculture contributed to markedly reduce the amount of nutrients coming from  
50 river run-off (Nausch et al. 1999; Carstensen et al. 2006; Rydberg et al. 2006). However, these  
51 efforts in decreasing nutrient loads have not resulted in improved water quality, due to the long  
52 time scales of biogeochemical cycles to reach equilibrium in the Baltic Sea region (Gustafsson et  
53 al. 2012). The Öresund, like most of the Baltic Sea, is still assessed to be eutrophic, and hypoxic  
54 events are frequent (Rosenberg et al. 1996; Conley et al. 2007, 2011; HELCOM 2009;  
55 Wesslander et al. 2016). Moreover, increasing temperatures and declining pH, linked to global  
56 climate change and ocean acidification, have been reported for surface and bottom waters in the  
57 area (Andersson et al. 2008; Göransson 2017). As a result, ecosystems in the Öresund are  
58 currently under the combined impact of natural and anthropogenic stressors (Henriksson 1969;  
59 Göransson et al. 2002; HELCOM 2009; ICES 2010). The multiple stressors currently affecting  
60 the environment make this region particularly interesting to study, and also highlight the need to  
61 obtain records of decadal and centennial environmental changes. As noted above, both recent  
62 human-induced impacts and climate variability have been substantial in the region. Therefore the  
63 question arises whether these factors have affected the benthic environment. Furthermore,  
64 sediment records of past environmental changes can provide crucial context for ongoing and  
65 future predicted changes in the Öresund and Baltic Sea regions.

66 We used the marine sediment record and its contents of foraminifera as well as sediment  
67 geochemistry to obtain records of decadal environmental changes. Benthic foraminifera are  
68 widely used for environmental reconstructions, based on their rapid response to environmental



69 changes, broad distribution, high densities, and often well-preserved tests (shells) in the sediment  
70 (e.g. Sen Gupta 1999). For instance, distribution of benthic foraminifera have been used for  
71 historical environmental reconstructions of fjords on decadal to centennial timescales on the  
72 Swedish west coast (Nordberg et al. 2000; Filipsson and Nordberg 2004a, 2004b; Polovodova  
73 Asteman and Nordberg 2013; Polovodova Asteman et al. 2015), and in the Kattegat  
74 (Seidenkrantz 1993; Christiansen et al. 1996). In the Öresund, living foraminiferal assemblages  
75 have been studied (Hansen 1965; Charrieau et al. 2018), but to the best of our knowledge, no  
76 studies of past foraminiferal assemblages have been performed. In this study, we used  
77 foraminiferal fauna analysis in combination with sediment geochemistry and grain-size analyses  
78 to reconstruct the environmental conditions of benthic systems during the last two centuries in  
79 the Öresund. Furthermore, we analyzed long time series of wind conditions in the area to  
80 evaluate the coupling between local changes in ecosystem variables and variations in  
81 atmospheric and subsequent hydrographic conditions, and a possible link with large-scale  
82 variations expressed through the North Atlantic Oscillation (NAO) index. Finally, we compared  
83 our data with the model ECOSMO II (Daewel and Schrum 2013; 2017) of currents and water  
84 circulation changes in the Öresund area during the period 1948–2013.

85 2 – Study site

86 The Öresund is a 118 km long narrow strait (Figure 1). The water depth in the northern part is on  
87 average 24 m but it reaches 53 m south of the Island of Ven. The Öresund is an important link  
88 between the North Sea, Skagerrak, Kattegat and the Baltic Sea (Figure 1), and up to 30 % of the  
89 water exchange in the region goes through the Öresund (Sayin and Krauß 1996; Leppäranta and  
90 Myrberg 2009); the remaining part goes through the Great and Little Belt. The width of the  
91 Öresund varies between 4 and 28 km, and the water has overall high current velocities, up to 1.5



92 m.s<sup>-1</sup> at the upper water layer in the northern part (Nielsen 2001). The fully marine Skagerrak  
93 consists of water masses from the North Sea and the North Atlantic and in general a thin surface  
94 layer with water originating from the Baltic Sea and rivers draining into the sea; the water  
95 circulation forms a cyclonic gyre (cf. Erbs-Hansen et al. 2012). Part of the Skagerrak waters  
96 reach the Kattegat and the Baltic Sea, where they are successively diluted with the large amounts  
97 of freshwater (around 15,000 m<sup>3</sup>/s, Bergström and Carlsson 1994) draining into the Baltic Sea  
98 from numerous large rivers. The low-saline Baltic Sea surface water is transported by the Baltic  
99 Current, which is typically confined along the Swedish west coast in the Kattegat but may cover  
100 a larger surface area towards the west, depending on wind direction. The Baltic Current later  
101 joins the Norwegian Coastal Current in the Skagerrak (Figure 1). The large fresh water input and  
102 the subsequent large salinity difference between the Kattegat and Baltic Sea result in a two-layer  
103 structure in the Öresund (Figure 2) (She et al. 2007; Leppäranta and Myrberg 2009). The water  
104 stratification is influenced by the surface water from Arkona Basin (salinity 7.5–8.5), the  
105 surface water from the Kattegat upper layer (salinity 18–26) and the lower layer of the Kattegat  
106 (salinity 32–34).

107 Salinity, temperature, pH, [O<sub>2</sub>] and nutrient content, here represented by dissolved inorganic  
108 nitrogen concentration [DIN] (nitrate + nitrite + ammonium), in the surface and bottom waters of  
109 the Öresund vary seasonally (Figure 3, Appendix A). In the surface and bottom water, salinity  
110 ranges between ~8 and ~18 and between ~29 and ~34, respectively, and it is more stable between  
111 April and July, when the stratification is the strongest (Figure 3). Temperature ranges between  
112 ~1 °C in February and ~19 °C in July in the surface water, while in the bottom water, the lowest  
113 temperature is found in March—April with ~5° C, and the highest temperature in October—  
114 November with ~13 °C. The pH varies between ~8.1 and ~8.6 in the surface water, and between



115 ~7.8 and ~8.6 in the bottom water, without a clear seasonal pattern (Figure 3).  $[O_2]$  in the bottom  
116 water reaches  $\sim 7 \text{ mL.L}^{-1}$  in January, and it is typically below  $2 \text{ mL.L}^{-1}$  in October, approaching  
117 hypoxic values. In the surface water,  $[DIN]$  can reach  $\sim 7 \text{ } \mu\text{mol.L}^{-1}$  in January, and it is  $\sim 0$   
118  $\mu\text{mol.L}^{-1}$  between April and August (Figure 3).

119 3 - Materials and Methods

120 3.1 Sampling

121 A suite of sediment cores, as well as water samples from the water column, were collected in  
122 November 2013 during a cruise with r/v *Skagerak*. Here we present the data from two sediment  
123 cores sampled at the Öresund station DV-1 ( $55^{\circ}55.59' \text{ N}$ ,  $12^{\circ}42.66' \text{ E}$ ) (Figure 1), north of the  
124 Island of Ven. The water depth was 45 m, and CTD casts were taken to measure salinity,  
125 temperature and  $[O_2]$  in the water column. Water samples were collected at 10, 15, 20, 30 and 43  
126 m from the Niskin bottles for carbonate chemistry analyses. The CTD and carbonate chemistry  
127 data are presented in Charrieau et al. (2018). The salinity profile in the water column showed the  
128 typical halocline at 10 m depth (Figure 2). The temperature and  $[O_2]$  decreased with depth. The  
129 pH values decreased with depth and increase again when reaching the bottom water (Figure 2).  
130 In general, it is challenging to obtain sediment cores in the Öresund, due the high current  
131 velocities up to  $1.5 \text{ m.s}^{-1}$  (Nielsen 2001), human-induced disturbances, and limited areas of  
132 recent sediment deposition (Lumborg 2005), but our site north of Ven represents an  
133 accumulation area. The cores (9-cm-inner-diameter) were collected using a GEMAX twin barrel  
134 corer. The corer allowed sampling of 30 and 36 cm long sediment cores (referred in this study as  
135 core DV1-G and DV1-I, respectively), which were sliced into one centimeter sections. The  
136 samples from the DV1-G core were analyzed for carbon and nitrogen content, grain size



137 distribution, and dated using Gamma spectroscopy. The samples from the DV1-I core were  
138 analyzed with respect to foraminiferal fauna and carbon and nitrogen content. The distinct  
139 carbon content profiles, measured on both cores, were used to correlate the  $^{210}\text{Pb}$  dated DV1-G  
140 core to the DV1-I core used for foraminiferal analyses.

141 3.2 Chronology

142 The age-depth model was established using  $^{210}\text{Pb}$  and  $^{137}\text{Cs}$  techniques on samples from the  
143 DV1-G core. The samples were measured with an ORTEC HPGe (High-Purity Germanium)  
144 Gamma Detector at the Department of Geology at Lund University, Sweden. Corrections for  
145 self-absorption were made for  $^{210}\text{Pb}$  following Cutshall et al. (1983). The instruments were  
146 calibrated against in-house standards and the maximum error was 0.5 year in the measurements.  
147 Excess (unsupported)  $^{210}\text{Pb}$  was measured down to 23 cm and the age model was calculated  
148 based on the Constant Rate of  $^{210}\text{Pb}$  Supply (CRS) model (Appleby 2001).

149 3.3 Foraminifera analyses

150 The foraminiferal samples were prepared following standard micropalaeontological techniques  
151 (e.g. Murray 2006). Approximately 10 g of freeze-dried sediment per sample were wet sieved  
152 thought a 63- $\mu\text{m}$  mesh screen and dried on filter paper at room temperature. Subsequently, the  
153 samples were dried sieved through 100- and 500- $\mu\text{m}$  mesh screens and separated into the  
154 fractions 100-500  $\mu\text{m}$  and  $>500$   $\mu\text{m}$ . The foraminifera from every second centimeter of the core -  
155 plus from additional centimeters around key zones - were picked and sorted under a Nikon  
156 microscope. A minimum of 300 specimens per sample were picked and identified, if necessary  
157 the samples were split with an Otto splitter (Otto 1933). For taxonomy at the genus level, we  
158 mainly followed Loeblich and Tappan (1964) with some updates from more recent literature, e.g.



159 Tappan and Loeblich (1988). For taxonomy at the species level, we mainly used Feyling-  
160 Hanssen (1964), Feyling-Hanssen et al. (1971) and Murray and Alve (2011). For original  
161 descriptions of the species, see Ellis and Messina (1940 and supplements up to 2013).  
  
162 Recently, the eastern Pacific morphospecies *Nonionella stella* has been presented as an invasive  
163 species in the Skagerrak-Kattegat region (Polovodova Asteman and Schönfeld 2015). However,  
164 a comparison of *N. stella* DNA sequences from the Santa Barbara Basin (USA) (Bernhard et al.  
165 1997) with the Swedish west coast specimens demonstrates that they represent two closely  
166 related species but are not conspecific (Deldicq et al. in press). Therefore, we have referred to the  
167 species found here as *Nonionella* sp. T1, following Deldicq et al. (in press). The species  
168 *Verneuilina media* (here referred to the genus *Eggerelloides*), which has often been reported in  
169 previous studies from the Skagerrak-Kattegat area (e.g. Conradsen et al. 1994), was  
170 morphologically close to *Eggerelloides scabrus* in the present material, and these two species  
171 have been grouped as *E. medius/scabrus*. The taxon *Elphidium excavatum* forma *clavata* (cf.  
172 Feyling-Hanssen 1972), was referred to as *Elphidium clavatum* following Darling et al. (2016).  
173 *Elphidium clavatum* and *Elphidium selseyense* (Heron-Allen and Earland) were morphologically  
174 difficult to separate in this region, as transitional forms occur. The dominant species was *E.*  
175 *clavatum*, but we acknowledge that a few individuals of *E. selseyense* could have been included  
176 in the counts. The taxon *Ammonia beccarii* was referred to as *Ammonia batava*, following recent  
177 molecular work done on the taxon *Ammonia* in the Kattegat region (Groeneveld et al., 2018; Bird  
178 et al. in press).  
  
179 Foraminiferal density was calculated and normalized to the number of specimens per 50 cm<sup>3</sup>.  
180 Data of densities of living + dead foraminifera for the first two centimeters of the core are from  
181 Charrieau et al. (2018). Some specimens displayed decalcified tests, however the inner organic



182 linings were preserved. These inner organic linings were reported separately and not included in  
183 the total foraminiferal counts. Benthic foraminiferal accumulation rates were calculated as  
184 follows:

185 
$$\text{BFAR (number of specimens.cm}^{-2}.\text{yr}^{-1}) = \text{BF} \times \text{SAR},$$

186 where BF is the number of benthic foraminifera per  $\text{cm}^3$  and SAR is the sediment accumulation  
187 rate ( $\text{cm}.\text{yr}^{-1}$ ). Foraminiferal species that accounted for >5 % of the total fauna in at least one of  
188 the samples were considered as major species, and their density was used in statistical analysis.  
189 To determine foraminiferal zones, stratigraphically constrained cluster analysis was performed,  
190 using the size-independent Morisita's index to account for the large differences in the densities  
191 between samples. A dendrogram was then constructed based on arithmetic averages with the  
192 UPGMA method (Unweighted Pair Group Method with Arithmetic Mean). Correspondence  
193 analysis was also performed, to determine significant foraminiferal species in each zone.  
194 Statistical analyses were performed using the PAST software (Hammer et al. 2001).

195 3.4 Organic matter analyses

196 Total Organic Carbon (TOC) and Total Nitrogen (TN) content were measured for both DV1-G  
197 and DV1-I. Approximately 8 mg of freeze-dried sediment was homogenized for each centimeter  
198 and placed in silver capsules. Removal of inorganic carbon was carried out by in-situ  
199 acidification (2M HCl) method based on Brodie et al. (2011). TOC and TN content were  
200 analyzed on a Costech ECS 4010 Elemental Analyzer at the Department of Geology, Lund  
201 University. The instrument was calibrated against in-house standards. The analytical precisions  
202 showed a reproducibility of 0.2 % and 0.03 % for TOC and TN contents, respectively. The molar  
203 C/N ratio was calculated.



204 3.5 Grain-size analyses

205 Grain-size analyses were performed on core DV1-G using 3.5 to 5 g of freeze-dried sediment for  
206 each centimeter. Organic matter was removed by adding 15 mL of 30 % H<sub>2</sub>O<sub>2</sub> and heating  
207 during 3 to 4 minutes until the reaction ceased. After the samples had cooled down, 10 mL of  
208 10 % HCl was added to remove carbonates; thereafter the sediment was washed with milli-Q  
209 until its pH was neutral. In the last step, biogenic silica was removed by boiling the sediment in  
210 100 mL 8 % NaOH, and then washed until neutral pH was reached. The sand fraction (>63 µm)  
211 was separated by sieving and the mass fraction of sand of each sample was calculated. Grain  
212 sizes <63 µm were analyzed by laser diffraction using a Sedigraph III Particle Size Analyzer at  
213 the Department of Geology, Lund University. The data were categorized into three size groups,  
214 <4 µm (clay), 4–63 µm (silt) and 63–2000 µm (sand).

215 3.6 Climate data and numerical modeling

216 Data from the dataset High Resolution Atmospheric Forcing Fields (HiResAFF) covering the  
217 time period 1850–2008 (Schenk and Zorita 2012; Schenk 2015) were used to study the variations  
218 of near-surface (10 m) wind conditions during the winter half of the year (October to March).  
219 The daily dataset can be downloaded from WDC Climate (Schenk 2017). Wind conditions over  
220 the Öresund are represented by the closest grid point of HiResAFF at 55° N and 12.5° E. The  
221 NAO index as defined by Jones et al. (1997) for boreal winter (December to March) was used,  
222 with updates taken from the Climate Research Unit (CRU,  
223 <https://crudata.uea.ac.uk/cru/data/nao/>). To allow comparison, the NAO and wind data were  
224 normalized relative to the period 1850–2008. Changes in the currents through the Öresund and  
225 the Kattegat were taken from the fully coupled physical biogeochemical model ECOSMO II



226 (Daewel and Schrum 2013, 2017), which was forced by NCEP/NCAR reanalysis data and covers  
227 the period 1950–2013. On model ECOSMO II, the simulated South-North currents are  
228 represented as VAV (vertically averaged V- component) and the simulated West-East currents as  
229 UAV (vertically averaged U - component).

230 4 – Results

231 4.1 Age model

232 The unsupported  $^{210}\text{Pb}$  showed a decreasing trend with depth in the DV1-G core (Figures 4A,  
233 4B). The peak observed in the  $^{137}\text{Cs}$  around 9 cm corresponds to the Chernobyl accident in 1986  
234 (Figure 4C). The unsupported  $^{210}\text{Pb}$  allowed direct dating of the core between 2013 and 1913.  
235 The sedimentation rate ranged between 1 and 5.6  $\text{mm.y}^{-1}$ , with an average of 2.2  $\text{mm.y}^{-1}$ , and  
236 was decreased with depth. The ages of the lower part of the sediment record were deduced by  
237 linear extrapolation based on a sedimentation rate of 1.4  $\text{mm.y}^{-1}$ , corresponding to the linear  
238 mean sedimentation rate between the years 1913 and 1946 (Figure 4D).

239 4.2 Foraminiferal assemblages and sediment features

240 The foraminiferal assemblages were composed of 76 species from the porcelaneous, hyalines  
241 and agglutinated forms (Appendix B). Eleven foraminiferal species had relative abundance  
242 higher than 5 % in at least one sample and were considered as major species (Plate 1, Figure 5).

243 The cluster analysis reveals three main foraminiferal zones (FOR-A, FOR-B, and FOR-C),  
244 separated into five subzones to which we assigned dates according to the age model: FOR-A1  
245 (1807–1870), FOR-A2 (1870–1953), FOR-B1 (1953–1998), FOR-B2 (1998–2009), and FOR-C  
246 (2009–2013) (Figures 5, 6). The correspondence analysis resulted in three factors explaining



247 92 % of the variance, and in assemblages consisting in seven significant species, presented in  
248 order of contribution: *Nonionella* sp. T1, *Nonionoides turgida*, *Ammonia batava*, *Stainforthia*  
249 *fusiformis*, *Elphidium albiumbilicatum*, *E. clavatum* and *Elphidium magellanicum* (Table 1).

250 421. Zone FOR-A1 (1807–1870)

251 The foraminiferal accumulation rate (BFAR) was on average  $5 \pm 3$  specimens.cm $^{-2} \cdot y^{-1}$  in zone  
252 FOR-A1 (Figure 5). The Shannon index was stable and low, around  $1.77 \pm 0.1$  (Figure 5). The  
253 agglutinated species *Eggerelloides medius/scabrus* and the hyaline species *Stainforthia*  
254 *fusiformis* made major contributions to the assemblages (relative abundances up to 53 % and  
255 34 %, respectively; Figure 5A). *Ammonia batava*, the three *Elphidium* species (*E.*  
256 *albiumbilicatum*, *E. clavatum*, and *E. magellanicum*), *Nonionellina labradorica* and the  
257 agglutinated species *Reophax subfusiformis* were also major species with abundances up to 7 %.  
258 The TOC and C/N values on this period were stable and were on average 3.36 % and 8.8 %,  
259 respectively (Figure 7). The clay size fraction dominated the sediment at the end of this period  
260 with a mean value of 63 %, and the sand content was around 7 % (Figure 7).

261 422. Zone FOR-A2 (1870–1953)

262 The BFAR was on average  $9 \pm 5$  specimens.cm $^{-2} \cdot y^{-1}$  in zone FOR-A2 (Figure 5). The Shannon  
263 index was stable and low, around  $1.94 \pm 0.15$  (Figure 5). *Stainforthia fusiformis* dominated the  
264 assemblage with relative abundances up to 56 % and BFAR up to 608 specimens.cm $^{-2} \cdot y^{-1}$   
265 (Figures 5A, 5B), which is the highest BFAR observed for this species along the core.  
266 *Eggerelloides medius/scabrus* was still very abundant, up to 48 % (Figure 5A). *Ammonia batava*,  
267 the three *Elphidium* species and *N. labradorica* were present but with lower abundances than in  
268 the zone FOR-A1 (maximum 5 %). *Bulimina marginata* started to be more abundant with an



269 average relative abundance of 2 % in the zone. *Reophax subfusiformis* was still a part of the  
270 assemblage and ranged between 1 and 8 %. The TOC and C/N values were stable and were on  
271 average 3.5 % and 8.74 %, respectively (Figure 7). The clay size fraction dominated the  
272 sediment during this period with a mean value of 63 %, and the sand content was around 6 %  
273 (Figure 7).

274 423. Zone FOR-B1 (1953–1998)

275 The BFAR increased massively during the zone FOR-B1 with on average  $54 \pm 31$  specimens.cm $^{-2} \cdot y^{-1}$   
276 and with a peak at 93 specimens.cm $^{-2} \cdot y^{-1}$  around 1965 (Figure 5). It is lower during the  
277 second part of the zone. The Shannon index was higher than in previous zones and it  
278 progressively increased towards the top of the zone (Shannon index average  $2.34 \pm 0.3$ ) (Figure  
279 5). The highest BFAR along the core were observed for all the dominant species of the previous  
280 zone FOR-A2, except for *S. fusiformis* (Figure 5B). The zone was then also characterized by a  
281 drastic drop in the relative abundance of *S. fusiformis* from 31 to 2 % (Figure 5A).  
282 *Eggerelloides medius/scabrus* gradually decreased in the zone, with relative abundances from  
283 49 to 24 %. The highest relative abundance of *A. batava* for the entire record was in this zone but  
284 it was slowly decreasing as well, from 10 to 3 %. The *Elphidium* group was more abundant than  
285 in the FOR-A zones and their relative abundance was increasing, especially for *E. clavatum*  
286 (increasing up to 23 %). *Bulimina marginata*, *N. labradorica* and *R. subfusiformis* had a relative  
287 abundance between 2 and 6 %. A period of lower TOC values was observed during zone FOR-  
288 B1 between 1953 and 1981, with an average of 2.38 % (Figure 7). On the same period, the sand  
289 content showed a pronounced increase, with an average of 24 % (Figure 7).

290 424. Zone FOR-B2 (1998–2009)



291 In zone FOR-B2 the BFAR was still high, on average  $55 \pm 6$  specimens.cm $^{-2} \cdot$ y $^{-1}$  (Figure 5). The  
292 Shannon index was high with an average of  $2.8 \pm 0.2$  (Figure 5). The dominant species in the  
293 zone were *E. clavatum* (up to 25 %) and *Eggerelloides medius/scabrus* (up to 15 %; Figure 5A).  
294 The other two *Elphidium* species reached their highest relative abundances over the core (up to  
295 6 %). *Nonionella* sp. T1, which had not occurred in the record until now, appeared in this zone  
296 with a relative abundance of 1 %. *Nonionoides turgida*, which was present in very low  
297 abundances along the core, had a mean abundance of 1 % in the zone (Figure 6A). *Stainforthia*  
298 *fusiformis* was present with up to 9 % in relative abundance and a BFAR higher than in zone  
299 FOR-B1 (up to 570 specimens.cm $^{-2} \cdot$ y $^{-1}$ ). *Ammonia batava*, *B. marginata*, *N. labradorica*, and *R.*  
300 *subfusiformis* were present and ranged between 2 and 8 %. The TOC values were increasing,  
301 with on average 3.05 % (Figure 7). The sediment was dominated by the clay fraction that was  
302 increasing (mean value of 58 %), and the sand content was around 17 % (Figure 7).

303 425. Zone FOR-C (2009–2013)

304 The BFAR was lower than in previous zones FOR-B1 and FOR-B2, with on average  $21 \pm 5$   
305 specimens.cm $^{-2} \cdot$ y $^{-1}$  (Figure 5). The Shannon index was the highest during FOR-C (Shannon  
306 index average  $2.93 \pm 0.07$ ) (Figure 5). *Nonionella* sp. T1 was a dominant specie in the zone with  
307 a strong increase in relative abundance (from 1 to 14 %) and in BFAR (from 61 to 137  
308 specimens.cm $^{-2} \cdot$ y $^{-1}$ ) (Figures 5A, 5B). *Elphidium clavatum* and *R. subfusiformis* were also  
309 dominant species with abundances up to 13%. *Nonionoides turgida* had its highest relative  
310 abundance and BFAR over the core during the zone, with up to 9 % and 342 specimens.cm $^{-2} \cdot$ y $^{-1}$ ,  
311 respectively (Figures 5A, 5B). *Eggerelloides medius/scabrus* had its lowest relative abundance  
312 over the core (up to 9 %). *Bulimina marginata*, the other two *Elphidium* species, *N. labradorica*  
313 and *S. fusiformis* were still present (between 1 and 6 %), while *Ammonia batava* was absent



314 during the zone. The TOC and C/N values were on average 3.71 % and 8.17 %, respectively  
315 (Figure 7). The clay size fraction dominated the sediment with a mean value of 66 % and the  
316 sand fraction was 7 % (Figure 7).

317 426. Inner organic linings

318 Decalcified specimens were few and ranged between 0 and 4 specimens.cm<sup>-2</sup>.y<sup>-1</sup> with an average  
319 of 1 specimen.cm<sup>-2</sup>.y<sup>-1</sup> (Fig. 5). They were observed throughout the core and especially during  
320 zone FOR-B2, and the morphology of the remaining inner organic linings allowed the  
321 identification of the taxon *Ammonia* (Plate 1).

322 4.3 Simulated data from model ECOSMO II

323 The VAV (vertically averaged South-North current velocity) through the Öresund from the  
324 model ECOSMO II showed a reversed pattern compared to the UAV (vertically averaged West-  
325 East current velocity) through the Kattegat (Figure 8). Thus, higher VAV through the Öresund  
326 translates to an increase in the East to West flow in the Kattegat (lower UAV), suggesting a  
327 stronger outflow from the Baltic Sea. The VAV through the Öresund had the lowest values  
328 around 1955 (Figure 8), followed by a shift to very high values, which dominated throughout  
329 1960–70. A comparable period with increased outflow from the Baltic into the Kattegat re-  
330 occurred during the period 1993–2000.

331 5 – Discussion

332 Our environmental interpretations of the foraminiferal assemblages were based on the ecological  
333 characteristics of each major species (Table 2). Based on our environmental reconstructions, we  
334 could infer environmental changes regarding [O<sub>2</sub>], salinity, organic matter content, and pollution



335 levels. Furthermore, we linked local environmental changes to larger atmospheric and  
336 hydrographic conditions.

337 5.1. 1807 – 1870

338 All the major species found in this period are tolerant to low oxygen conditions, especially the  
339 two main species: *S. fusiformis* and *E. medius/scabrus* (Table 2). *Stainforthia fusiformis* is an  
340 opportunistic species used to hypoxic and potentially anoxic conditions (Alve 1994), and *E.*  
341 *medius/scabrus* specimens have been found alive down to 10 cm in the sediment, where no  
342 oxygen was available (Cesbron et al. 2016). *Stainforthia fusiformis* and *N. labradorica* are also  
343 able to denitrify (Piña-Ochoa et al. 2010). The fact that species tolerant to low oxygen conditions  
344 dominated, and the presence of species that have the capacity to denitrify, suggest that low  
345 oxygen conditions were prevailing during this period. Furthermore, *S. fusiformis* prefers organic  
346 rich substrate and clayey sediment, which was measured in our core during this time period  
347 (Figure 7). The low species diversity, as indicated by the low Shannon index in this section of  
348 the core, is usually linked with low salinity (Sen Gupta 1999a). Most of the major species found  
349 during this period, such as the *Elphidium* group, *R. subfusiformis* and *A. batava* tolerate lower  
350 salinities, and are typical of brackish environments (Table 2). The low occurrence of *B.*  
351 *marginata*, a typical marine species, also suggests a salinity lower than in the open ocean.  
352 However, the salinity was probably not below 30, which is the lower limit for *N. labradorica* and  
353 *S. fusiformis*, which were present throughout the period (Figure 5, Table 2). In summary, this  
354 period appears to have been characterized by low [O<sub>2</sub>], high organic matter content, and salinity  
355 around 30.

356 5.2 1870 – 1953



357 *Stainforthia fusiformis* was largely dominating the assemblage during this period, which may  
358 suggest even lower oxygen conditions than during the previous period. This would also go along  
359 with the low species diversity, which is usually linked to low salinity. However, the occurrence  
360 of the marine species *B. marginata* suggests that the salinity was at least 32. Low oxygen is  
361 frequently associated with high organic matter contents, since oxygen is consumed during  
362 remineralization of organic matter. The TOC levels observed in our core in this zone were high,  
363 but not higher than in the previous zone (Figure 7). At the time of the industrial revolution, the  
364 Öresund was used as a sewage recipient for a mixture of domestic and industrial wastes,  
365 industrial cooling water and drainage water (Henriksson 1968), and the amount of marine traffic  
366 increased considerably during this time period. This diverse type of pollution could have  
367 modified the water properties, for example regarding the carbonate chemistry and pH. Indeed,  
368 this zone is characterized by the presence of organic linings in the core (see also section 5.6).  
369 Moreover, heavy metals, fuel ash (black carbon) and pesticides have been demonstrated to  
370 generally have a negative effect on foraminiferal abundance and diversity (Yanko et al. 1999).  
371 Pollution and low oxygen concentration could explain the low species BFAR and diversity as  
372 well as the dissolution of tests during this period. Other species that were present, i.e. the  
373 agglutinated species *E. medius/scabrus* and *R. subfusiformis*, are known to be tolerant to various  
374 kind of pollution (Table 2).

375 5.3 1953 – 1998

376 During this period, the large increase in the general BFAR could suggest that the specimens were  
377 not in situ, but transported into the area. In line with this is the coarser grain size observed during  
378 this period, indicating possible changes in the current system (Figure 7). However, the dating of  
379 our core showed continuous sediment accumulation without any interruption during this period



380 (Figure 4). Moreover, all the new dominating species were already present in the core, even if in  
381 lower relative abundances (Figure 5A). This indicates that the BFAR increase is most likely not  
382 due to specimens transport but rather as a result of a change in substrate and environmental  
383 conditions that became favorable for a different foraminiferal assemblage. The higher  
384 foraminiferal diversity compared to previous periods and the decrease in the relative abundance  
385 of *S. fusiformis* may indicate more oxic conditions. *Elphidium clavatum* has been found in coarse  
386 sediment in the area (Bergsten et al. 1996), and other species that tolerate sandy environments  
387 and varying TOC dominated the assemblage, such as *A. batava*, the other species in the  
388 *Elphidium* group, *B. marginata*, and *E. medius/scabrus*. Furthermore, anthropogenic activities  
389 such as agricultural practices were intensified during this period until the 1980s, which resulted  
390 in increased nutrient loads and resulting eutrophication (i.e. Rydberg et al. 2006). The increase in  
391 organic matter may have been beneficial for foraminifera as food source. Food webs and species  
392 interaction like intra and inter competition might also have been modified, giving the advantage  
393 to some species such as the *Elphidium* group to develop in these new environmental conditions.

394 The temporal coincidence with the shifts seen in the sediment record and the anomalous wind  
395 conditions suggests a notable change of the currents through the Öresund (Figures 8, 9). The  
396 simulated currents through the Öresund confirm such an abrupt change characterized by a shift  
397 from very limited outflow from the Baltic to the Kattegat before ~1960 to more than a decade of  
398 high relative outflow (high VAV) from the Öresund to the Kattegat and high current velocities  
399 (Figure 8). While the simulation only covers the period after 1950, the analysis of wind  
400 conditions and the NAO index suggest that the anomalies in the current and sediment pattern  
401 from ~mid 1950's might have been unprecedented since at least the middle of the 19<sup>th</sup> century  
402 (Figure 9). The shift in local sediment properties and the shift to higher BFAR and species



403 diversity suggest a combination of anomalous currents during a period of unusually negative  
404 NAO index and the abrupt first advection of anthropogenic eutrophication from the Baltic Sea  
405 towards the Kattegat. Consistent with our findings, long-term variations in Large Volume  
406 Changes in the Baltic Sea (LVS, Lehmann and Post 2015; Lehmann et al. 2017), which are  
407 calculated from >29 cm (~100 km<sup>3</sup>) daily sea-level changes at Landsort (58.74° N; 17.87° E) for  
408 1887–2015, show an unusual cluster of both, more frequent and also larger LVCs during the  
409 1970's to 1980's relative to the entire time period. Notably, this period coincides with the most  
410 dramatic shift in foraminiferal BFAR and species diversity as well as an increase in sand content.  
411 The period before the “regime shift” of the 1950's to 1960's is dominated by very infrequent and  
412 few large LVC events. After the shift, the 1990's show also very few or partly no LVC events  
413 with generally record-low Major Baltic Inflow events.

414 Thus, during this period, the ecosystems were affected both by climatic effects through  
415 sedimentation changes, and human impact. After ~1980, the general BFAR was lower during a  
416 short time (Figures 5, 9). This could be linked to the measures that were taken in agriculture and  
417 water treatments in order to reduce the nutrients discharge (Carstensen et al. 2006; Conley et al.  
418 2007), which could have reduced the food input. Interestingly, when the sedimentation pattern  
419 changes again and the sand content decreases markedly (Figure 7), the new species in the  
420 foraminiferal fauna do not return to previous relative abundances as one could have expected  
421 (Figure 5A). This suggests that once the foraminiferal fauna was established in the Öresund area  
422 after the ~1953 shift, it created a new state of equilibrium.

423 5.4 1998 – 2009



424 The foraminiferal assemblage in this zone was similar to the previous one, with high BFAR, high  
425 diversity, and the *Elphidium* group as dominating species. This period is, however, characterized  
426 by the appearance of two new major species: *N. turgida* and *Nonionella* sp. T1. *Nonionella* sp.  
427 T1 is suggested to be an invasive species in the region which arrived by ship ballast tanks around  
428 1985, and rapidly expanded to the Kattegat and Öresund (Polovodova Asteman and Schönfeld  
429 2015). According to our dated core, the species arrived in the Öresund ~2000 CE (Figure 5). The  
430 species is also present on the south coast of Norway since after 2009 (Deldicq et al., in press),  
431 but additional genetic analyses are necessary to have a better overview of the species' origin and  
432 expansion. *Nonionoides turgida* is an opportunistic species that prefers high levels of organic  
433 matter in the sediment, as observed in our core during this period (Figure 7). The increase in the  
434 *S. fusiformis* BFAR suggest lower [O<sub>2</sub>] than in the previous zone, which was indeed a general  
435 trend in the Danish waters during this time period (Conley et al. 2007). This period was then  
436 characterized by low [O<sub>2</sub>], high organic matter content, and open ocean salinity.

437 5.5 2009 – 2013

438 The ability of *Nonionella* sp. T1 to denitrify and its tolerance to varying environment may  
439 explain its rapid increase during this period. The increase of *N. turgida* also suggests higher  
440 levels of organic matter in the sediment. The dominance of these two species and the lower  
441 BFAR compared to previous periods suggest low oxygen levels. This period is thus characterized  
442 by low [O<sub>2</sub>], high organic matter content, and open ocean salinity.

443 5.6 Dissolution

444 The inner organic linings of the taxon *Ammonia* were observed (in low numbers, < 5 units) along  
445 the whole core, except in the top two centimeters (Figure 5). Inner organic linings of the taxa



446 *Ammonia* and/or *Elphidium* were noticed in previous studies among dead fauna in the region  
447 (Jarke 1961; Hermelin 1987: Baltic Sea; Christiansen et al. 1996; Murray and Alve 1999:  
448 Kattegat and Skagerrak; Filipsson and Nordberg 2004b: Koljö Fjord). Dissolution of calcareous  
449 foraminiferal tests has been considered as a taphonomic process, affecting the test of the  
450 specimens after their death (Martin 1999; Berkeley et al. 2007). However, living decalcified  
451 foraminifera have been observed in their natural environment in the south Baltic Sea (Charrieau  
452 et al. 2018) and the Arcachon Bay, France (Cesbron et al. 2016) and, proving that test dissolution  
453 can also occur while the specimens live. In any case, low pH and low calcium carbonate  
454 saturation are suggested as involved in the observed dissolution (Jarke 1961; Christiansen et al.  
455 1996; Murray and Alve 1999; Cesbron et al. 2016; Charrieau et al. 2018). Test dissolution may  
456 occur in all calcitic species, but only the organic linings of *Ammonia* were found in our study,  
457 probably because these were more robust to physical stress such as abrasion.

458 6 – Conclusion

459 In this study, we described an environmental record from the Öresund, based on benthic  
460 foraminifera – and geochemical data and we link the results with reconstructed wind data, NAO  
461 index and current changes model. Five foraminiferal zones were differentiated and associated  
462 with environmental changes in terms of salinity,  $[O_2]$ , and organic matter content. The main  
463 event is a major shift in the foraminiferal assemblage ~1950, when the BFAR massively  
464 increased and *S. fusiformis* stopped dominating the assemblage. This period also corresponds to  
465 an increase in grain-size, resulting in a higher sand content. The grain-size distribution suggests  
466 changes in the current velocities which are confirmed by simulated current velocity through the  
467 Öresund. Human activities through increased eutrophication also influenced the foraminiferal



468 fauna changes during this period. Organic linings of *Ammonia* were observed throughout the  
469 core, probably linked to low pH and calcium carbonate saturation, affecting test preservation.  
  
470 The long-term reconstruction of sediment – and ecosystem parameters since ~1807 suggests that  
471 the onset of increased anthropogenic eutrophication of the eastern Kattegat started with an abrupt  
472 shift ~1960 during a period of strongly negative NAO. With unusually calm wind conditions  
473 during the winter half and increased easterly winds, the conditions were ideal for larger Baltic  
474 outflow invents which then allowed more frequent and larger Baltic inflow events, as calculated  
475 from LVC events during this period. The sediment record with unprecedented high temporal  
476 resolution points towards the importance of considering also large Baltic outflow events to the  
477 Kattegat which have a large impact at least at Ven Island and possibly larger parts of the  
478 Kattegat. Because the Baltic Sea has much higher eutrophication levels and less oxygenated and  
479 less saline waters, larger outflow events may have a significant impact also on the Kattegat.  
  
480 Periods with negative NAO or conditions with intense atmospheric blocking over Scandinavia  
481 like 2018 may also increase the influence of Baltic Sea problems on the Kattegat region.

482 Acknowledgments

483 We would like to thank the captain and the crew of the r/v *Skagerak*. We acknowledge Git  
484 Klintvik Ahlberg for the assistance in the laboratory, Yasmin Bokhari Friberg and Åsa Wallin  
485 for the help with the grain-size analysis, and Guillaume Fontorbe for help with the age model.  
486 The hydrographic data used in the projected is collected from SMHI's data base SHARK. The  
487 SHARK data collection is organized by the environmental monitoring program and funded by  
488 the Swedish Environmental Protection Agency. The study was financially supported by the



489 Swedish Research Council FORMAS (grants 2012-2140 and 217-2010-126), the Royal  
490 Physiographic Society in Lund and Oscar and Lili Lamm's Foundation.

491 Supplementary data

492 Appendix A with time series of salinity, temperature and dissolved oxygen concentration at the  
493 bottom water of the Öresund and Appendix B with total foraminiferal faunas normalized to 50  
494 cm<sup>3</sup> along the DV core are available in the online version of the article.

495 References

496 Alve, E. « Opportunistic Features of the Foraminifer *Stainforthia Fusiformis* (Williamson): Evidence  
497 from Frierfjord, Norway ». *Journal of Micropalaeontology* 13 (1): 24-24.  
498 <https://doi.org/10.1144/jm.13.1.24>. 1994.

499 Andersson, P., B. Häkansson, J. Häkansson, and E. Sahlsten. « SMHI Report: Marine acidification - On  
500 effects and monitoring of marine acidification in the seas surrounding Sweden ». Report  
501 *Oceanography* No 92. 2008.

502 Appleby, P. G. « Chronostratigraphic techniques in recent sediments ». In *Tracking environmental change*  
503 using lake sediments, Last W. M. and Smol J. P. Vol. 1. Springer Netherlands.  
504 <http://www.springer.com/gp/book/9780792364825>. 2001.

505 Bergsten, H., K. Nordberg, and B. Malmgren. « Recent benthic foraminifera as tracers of water masses  
506 along a transect in the Skagerrak, North-Eastern North Sea ». *Journal of Sea Research* 35 (1-3):  
507 111-21. [https://doi.org/10.1016/S1385-1101\(96\)90740-6](https://doi.org/10.1016/S1385-1101(96)90740-6). 1996.

508 Bergström, S., and B. Carlsson. « River runoff to the Baltic Sea - 1950-1990 ». *Ambio* 23 (4-5): 280-87.  
509 1994.

510 Berkeley, A., C. T. Perry, S. G. Smithers, B. P. Horton, and K. G. Taylor. « A review of the ecological  
511 and taphonomic controls on foraminiferal assemblage development in intertidal environments ».  
512 *Earth-Science Reviews* 83 (3): 205-30. <https://doi.org/10.1016/j.earscirev.2007.04.003>. 2007.

513 Bernhard, J. M., B. K. Sen Gupta, and P. F. Borne. « Benthic foraminiferal proxy to estimate dysoxic  
514 bottom-water oxygen concentrations; Santa Barbara Basin, U.S. pacific continental margin ».  
515 *Journal of Foraminiferal Research* 27 (4): 301-10. <https://doi.org/10.2113/gsjfr.27.4.301>. 1997.

516 Bird, C., M. Schweizer, A. Roberts, W.E.N. Austin, K.L. Knudsen, K.M. Evans, H.L. Filipsson, M.D.J.  
517 Sayer, E. Geslin, and K.F. Darling. « The genetic diversity, morphology, biogeography, and  
518 taxonomic designations of *Ammonia* (Foraminifera) in the Northeast Atlantic ». *Marine  
519 Micropaleontology*. <https://doi.org/10.1016/j.marmicro.2019.02.001>. In press.

520 Brodie, C.R., M.J. Leng, J.S. L. Casford, C.P. Kendrick, J.M. Lloyd, Z. Yongqiang, and M.I. Bird.  
521 « Evidence for bias in C and N concentrations and  $\delta^{13}\text{C}$  composition of terrestrial and aquatic  
522 organic materials due to pre-analysis acid preparation methods ». *Chemical Geology* 282 (3-4):  
523 67-83. <https://doi.org/10.1016/j.chemgeo.2011.01.007>. 2011.

524 Carstensen, J., D. J. Conley, J. H. Andersen, and G. Årtebjerg. « Coastal eutrophication and trend  
525 reversal: A Danish case study ». *Limnology and Oceanography* 51 (1, part 2): 398-408. 2006.



526 Cesbron, F., E. Geslin, F. J. Jorissen, M. L. Delgard, L. Charrieau, B. Deflandre, D. Jézéquel, P. Anschutz,  
527 and E. Metzger. « Vertical distribution and respiration rates of benthic foraminifera: Contribution  
528 to aerobic remineralization in intertidal mudflats covered by *Zostera noltei* meadows ». *Estuarine,*  
529 *Coastal and Shelf Science* 179: 23–38. 2016.

530 Charrieau, L. M., H. L. Filipsson, K. Ljung, M. Chierici, K. L. Knudsen, and E. Kritzberg. « The effects  
531 of multiple stressors on the distribution of coastal benthic foraminifera: A case study from the  
532 Skagerrak-Baltic Sea region ». *Marine Micropaleontology* 139  
533 <https://doi.org/10.1016/j.marmicro.2017.11.004>. 2017.

534 Christiansen, C., H. Kunzendorf, M. J. C. Laima, L. C. Lund-Hansen, and A. M. Pedersen. « Recent  
535 changes in environmental conditions in the southwestern Kattegat, Scandinavia ». *NGU Bull.*, n°  
536 430: 137–44. 1996.

537 Conley, D., J. Cartensen, G. Årtebjerg, P. B. Christensen, T. Dalsgaard, J. L. S. Hansen, and A. B.  
538 Josefson. « Long-term changes and impacts of hypoxia in Danish coastal waters ». *Ecological*  
539 *Applications* 17 (5): S165–84. <https://doi.org/10.1890/05-0766.1>. 2007.

540 Conley, D. J., J. Carstensen, J. Aigars, P. Axe, E. Bonsdorff, T. Eremina, B.-M. Haahti, et al. « Hypoxia  
541 is increasing in the coastal zone of the Baltic Sea ». *Environmental Science & Technology* 45  
542 (16): 6777–83. <https://doi.org/10.1021/es201212r>. 2011.

543 Conradsen, K., H. Bergsten, K.L. Knudsen, K. Nordberg, and M.-S. Seidenkrantz. « Recent benthic  
544 foraminiferal distribution in the Kattegat and the Skagerrak, Scandinavia ». *Cushman Foundation*  
545 *Special Publication No.32*, 53–68. 1994.

546 Cutshall, N. H., I. L. Larsen, and C. R. Olsen. « Direct analysis of  $^{210}\text{Pb}$  in sediment samples: Self-  
547 absorption corrections ». *Nuclear Instruments and Methods in Physics Research* 206 (1): 309–12.  
548 [https://doi.org/10.1016/0167-5087\(83\)91273-5](https://doi.org/10.1016/0167-5087(83)91273-5). 1983.

549 Daewel, U., and C. Schrum. « Simulating long-term dynamics of the coupled North Sea and Baltic Sea  
550 ecosystem with ECOSMO II: Model Description and Validation ». *Journal of Marine Systems*  
551 119–120: 30–49. <https://doi.org/10.1016/j.jmarsys.2013.03.008>. 2013.

552 ———. « Low-frequency variability in North Sea and Baltic Sea identified through simulations with the  
553 3-D coupled physical–biogeochemical model ECOSMO ». *Earth System Dynamics* 8: 801–15.  
554 <https://doi.org/10.5194/esd-8-801-2017>. 2017.

555 Darling, K.F., M. Schweizer, K.L. Knudsen, K.M. Evans, C. Bird, A. Roberts, H.L. Filipsson, et al. « The  
556 genetic diversity, phylogeography and morphology of Elphidiidae (Foraminifera) in the Northeast  
557 Atlantic ». *Marine Micropaleontology*. <https://doi.org/10.1016/j.marmicro.2016.09.001>. 2016.

558 Deldicq, N., E. Alve, M. Schweizer, I. Polovodova-Asteman, S. Hess, K. Darling and V.M.P. Bouchet. «  
559 History of the introduction of a species resembling the benthic foraminifera *Nonionella stella* in  
560 the Oslofjord (Norway): morphological, molecular and paleo-ecological evidences ». *Aquatic*  
561 *Invasions* 14. In press.

562 Ellis, B. F., and A. R. Messina. Catalogue of Foraminifera. New York: Micropaleontology Press, The  
563 American Museum of Natural History. 1940.

564 Erbs-Hansen, D.R., K.L. Knudsen, A.C. Gary, R. Gyllencreutz, and E. Jansen. « Holocene climatic  
565 development in Skagerrak, Eastern North Atlantic: foraminiferal and stable isotopic evidence ».  
566 *The Holocene* 22 (3): 301–12. <https://doi.org/10.1177/0959683611423689>. 2012.

567 Feyling-Hanssen, R. W. Foraminifera in Late Quaternary Deposits from the Oslofjord Area. Vol. Issue  
568 225 of *Skrifter (Norges geologiske undersøkelse)*. Universitetsforlaget. 1964.

569 Feyling-Hanssen, R. W., J. A. Jørgensen, K. L. Knudsen, et A.-L. L. Andersen. Late quaternary  
570 foraminifera from Vendsyssel, Denmark and Sandnes, Norway. Vol. 21, 67–317. Issues 2-3 of  
571 *Bulletin of the Geological Society of Denmark*. Dansk geologisk forening. 1971.

572 Feyling-Hanssen, R.W. « The Foraminifer Elphidium excavatum (Terquem) and its variant forms ».  
573 *Micropaleontology* 18 (3): 337–54. <https://doi.org/10.2307/1485012>. 1972.



574 Filipsson, H.L., and K. Nordberg. « Climate variations, an overlooked factor influencing the recent  
575 marine environment. An example from Gullmar Fjord, Sweden, illustrated by Benthic  
576 Foraminifera and Hydrographic Data ». *Estuaries* 27 (5): 867–81. 2004a.  
577 ———. « A 200-Year Environmental Record of a Low-Oxygen Fjord, Sweden, Elucidated by Benthic  
578 Foraminifera, Sediment Characteristics and Hydrographic Data ». *The Journal of Foraminiferal  
579 Research* 34 (4): 277–93. <https://doi.org/10.2113/34.4.277>. 2004b.  
580 Göransson, P. « Changes of benthic fauna in the Kattegat – An indication of climate change at mid-  
581 latitudes? » *Estuarine, Coastal and Shelf Science* 194. <https://doi.org/10.1016/j.ecss.2017.06.034>.  
582 2017.  
583 Göransson, P., L. A. Angantyr, J. B. Hansen, G. Larsen, and F. Bjerre. « Öresunds bottenfauna ».  
584 Öresundsvattensamarbetet. 2002.  
585 Groeneveld, J., H. L. Filipsson, W.E.N. Austin, K. Darling, D. McCarthy, N.B.Q. Krupinski, C. Bird, and  
586 M. Schweizer. « Assessing proxy signatures of temperature, salinity and hypoxia in the Baltic Sea  
587 through foraminifera-based geochemistry and faunal assemblages ». *Journal of  
588 Micropalaeontology* 37: 403–29. <https://doi.org/10.5194/jm-37-403-2018>. 2018.  
589 Gustafsson, Bo G., Frederik Schenk, Thorsten Blenckner, Kari Eilola, H. E. Markus Meier, Bärbel  
590 Müller-Karulis, Thomas Neumann, Tuija Ruoho-Airola, Oleg P. Savchuk, and Eduardo Zorita.  
591 « Reconstructing the development of Baltic Sea eutrophication 1850–2006 ». *Ambio* 41 (6): 534–  
592 48. <https://doi.org/10.1007/s13280-012-0318-x>. 2012.  
593 Hammer, Ø., D.A.T. Harper, and P.D. Ryan. « PAST: Paleontological statistics software package for  
594 education and data analysis. » *Palaeontologia Electronica* 4 ((1)): 9pp. 2001.  
595 Hansen, H. J. « On the sedimentology and the quantitative distribution of living foraminifera in the  
596 northern part of the Øresund ». *Ophelia* 2 (2): 323–31.  
597 <https://doi.org/10.1080/00785326.1965.10409608>. 1965.  
598 HELCOM. « Eutrophication in the Baltic Sea – An integrated thematic assessment of the effects of  
599 nutrient enrichment and eutrophication in the Baltic Sea region. » *Balt. Sea Environ. Proc.* n°  
600 115B. 2009.  
601 Henriksson, R. « The bottom fauna in polluted areas of the Sound ». *Oikos* 19 (1): 111–25.  
602 <https://doi.org/10.2307/3564736>. 1968.  
603 ———. « Influence of pollution on the bottom fauna of the Sound (Øresund) ». *Oikos* 20 (2): 507–23.  
604 <https://doi.org/10.2307/3543212>. 1969.  
605 Hermelin, J.O.R. « Distribution of Holocene benthic foraminifera in the Baltic Sea ». *The Journal of  
606 Foraminiferal Research* 17 (1): 62–73. <https://doi.org/10.2113/gsjfr.17.1.62>. 1987.  
607 ICES. Integrated ecosystem assessments of seven Baltic Sea areas covering the last three decades.  
608 International Council for the Exploration of the Sea, Cooperative Research Report No. 302. 2010.  
609 Jarke, J. « Beobachtungen über Kalkauflösung an Schalen von Mikrofossilien in Sedimenten der  
610 westlichen Ostsee ». *Deutsche Hydrografische Zeitschrift* 14 (1): 6–11.  
611 <https://doi.org/10.1007/BF02226819>. 1961.  
612 Jones, P. D., T. Jonsson, and D. Wheeler. « Extension to the North Atlantic oscillation using early  
613 instrumental pressure observations from Gibraltar and South-west Iceland ». *International Journal  
614 of Climatology* 17: 1433–50. [https://doi.org/10.1002/\(SICI\)1097-0088\(19971115\)17:13<1433::AID-JOC203>3.0.CO;2-P](https://doi.org/10.1002/(SICI)1097-0088(19971115)17:13<1433::AID-JOC203>3.0.CO;2-P). 1997.  
615 Leppäranta, M., and K. Myrberg. *Physical Oceanography of the Baltic Sea*. Berlin, Heidelberg: Springer  
616 Berlin Heidelberg. 2009.  
617 Loeblich, A. R., and H. Tappan. « Part C, Protista 2, Sarcodina, Chiefly “Thecamoebians” and  
618 Foraminiferida ». In *Treatise on Invertebrate Paleontology*, Moore, R.C., 900 pp. The Geological  
619 Society of America and the University of Kansas. 1964.  
620 Lumborg, U. « Modelling the deposition, erosion, and flux of cohesive sediment through Øresund ».  
621 *Journal of Marine Systems* 56 (1): 179–93. <https://doi.org/10.1016/j.jmarsys.2004.11.003>. 2005.



623 Martin, R.E. « Taphonomy and Temporal Resolution of Foraminiferal Assemblages ». In *Modern*  
624 *Foraminifera*, 281-98. Springer Netherlands. [https://doi.org/10.1007/0-306-48104-9\\_16](https://doi.org/10.1007/0-306-48104-9_16). 1999.

625 Murray, J. W. *Ecology and applications of benthic foraminifera*. Cambridge University Press. 2006.

626 Murray, J. W., and E. Alve. « The distribution of agglutinated foraminifera in NW European seas:  
627 Baseline data for the interpretation of fossil assemblages ». *Palaeontologia Electronica* 14 (2):  
628 14A: 41p. 2011.

629 Murray, John W., and Elisabeth Alve. « Taphonomic experiments on marginal marine foraminiferal  
630 assemblages: how much ecological information is preserved? » *Palaeogeography, Palaeoclimatology,*  
631 *Palaeoecology* 149 (1-4): 183-97. [https://doi.org/10.1016/S0031-0182\(98\)00200-4](https://doi.org/10.1016/S0031-0182(98)00200-4). 1999.

632 Nausch, G., D. Nehring, and G. Aertebjerg. « Anthropogenic nutrient load of the Baltic Sea ».  
633 *Limnologica - Ecology and Management of Inland Waters* 29 (3): 233-41.  
634 [https://doi.org/10.1016/S0075-9511\(99\)80007-3](https://doi.org/10.1016/S0075-9511(99)80007-3). 1999.

635 Nielsen, M. H. « Evidence for internal hydraulic control in the northern Øresund ». *Journal of*  
636 *Geophysical Research* 106 (C7): 14,055-14,068. <https://doi.org/10.1029/2000JC900162>. 2001.

637 Nordberg, K., M. Gustafsson, and A.-L. Krantz. « Decreasing oxygen concentrations in the Gullmar Fjord,  
638 Sweden, as confirmed by benthic foraminifera, and the possible association with NAO ». *Journal*  
639 *of Marine Systems* 23 (4): 303-16. [https://doi.org/10.1016/S0924-7963\(99\)00067-6](https://doi.org/10.1016/S0924-7963(99)00067-6). 2000.

640 Otto, G.H. « Comparative tests of several methods of sampling heavy mineral concentrates ». *Journal of*  
641 *Sedimentary Research* 3 (1): 30-39. 1933.

642 Piña-Ochoa, E., S. Høgslund, E. Geslin, T. Cedhagen, N.P. Revsbech, L.P. Nielsen, M. Schweizer, F.  
643 Jorissen, S. Rysgaard, and N. Risgaard-Petersen. « Widespread occurrence of nitrate storage and  
644 denitrification among Foraminifera and Gromiida ». *Proceedings of the National Academy of*  
645 *Science* 107: 1148-53. <https://doi.org/10.1073/pnas.0908440107>. 2010.

646 Polovodova Asteman, I., D. Hanslik, and K. Nordberg. « An almost completed pollution-recovery cycle  
647 reflected by sediment geochemistry and benthic foraminiferal assemblages in a Swedish-  
648 Norwegian Skagerrak fjord ». *Marine Pollution Bulletin* 95 (1): 126-40.  
649 <https://doi.org/10.1016/j.marpolbul.2015.04.031>. 2015.

650 Polovodova Asteman, I., and K. Nordberg. « Foraminiferal fauna from a deep basin in Gullmar Fjord:  
651 The influence of seasonal hypoxia and North Atlantic Oscillation ». *Journal of Sea Research* 79:  
652 40-49. <https://doi.org/10.1016/j.seares.2013.02.001>. 2013.

653 Polovodova Asteman, I., and J. Schönfeld. « Recent invasion of the foraminifer *Nonionella stella*  
654 Cushman & Moyer, 1930 in northern European waters: Evidence from the Skagerrak and its  
655 fjords ». *Journal of Micropalaeontology* 35 (1). <https://doi.org/10.1144/jmpaleo2015-007>. 2015.

656 Rosenberg, R., I. Cato, L. Förlin, K. Grip, and J. Rodhe. « Marine environment quality assessment of the  
657 Skagerrak - Kattegat ». *Journal of Sea Research* 35 (1): 1-8. [https://doi.org/10.1016/S1385-1101\(96\)90730-3](https://doi.org/10.1016/S1385-1101(96)90730-3). 1996.

658 Rydberg, L., G. Aertebjerg, and L. Edler. « Fifty years of primary production measurements in the Baltic  
659 entrance region, trends and variability in relation to land-based input of nutrients ». *Journal of Sea*  
660 *Research* 56 (1): 1-16. <https://doi.org/10.1016/j.seares.2006.03.009>. 2006.

661 Sayin, E., and W. Krauß. « A numerical study of the water exchange through the Danish Straits ». *Tellus*,  
662 n° 48(2): 324-41. <https://doi.org/10.1034/j.1600-0870.1996.t01-1-00009.x>. 1996.

663 Schenk, F. « The analog-method as statistical upscaling tool for meteorological field reconstructions over  
664 Northern Europe since 1850 ». *Dissertation, University of Hamburg*. <http://ediss.sub.uni-hamburg.de/volltexte/2015/7156/>. 2015.

665 ———. « The long-term dataset of High Resolution Atmospheric Forcing Fields (HiResAFF) for  
666 Northern Europe since 1850 ». *World Data Center for Climate (WDCC) at DKRZ*.  
667 <https://doi.org/10.1594/WDCC/HiResAFF>. 2017.

668

669

670



671 Schenk, F., and E. Zorita. « Reconstruction of high resolution atmospheric fields for Northern Europe  
672 using analog-upscaling ». *Climate of the Past* 8: 1681–1703. <https://doi.org/10.5194/cp-8-1681-2012>. 2012.

673 Seidenkrantz, Marit-Solveig. « Subrecent changes in the foraminiferal distribution in the Kattegat and the  
674 Skagerrak, Scandinavia: Anthropogenic influence and natural causes ». *Boreas* 22 (4): 383–95.  
675 <https://doi.org/10.1111/j.1502-3885.1993.tb00201.x>. 1993.

676 Sen Gupta, B. K.. « Foraminifera in marginal marine environments ». In *Modern Foraminifera*, 141–59.  
677 Springer Netherlands. [https://doi.org/10.1007/0-306-48104-9\\_9](https://doi.org/10.1007/0-306-48104-9_9). 1999a  
678 ———. *Modern Foraminifera*. Springer Science & Business Media. 1999b.

679 She, Jun, Per Berg, and Jacob Berg. « Bathymetry impacts on water exchange modelling through the  
680 Danish Straits ». *Journal of Marine Systems, Marine Environmental Monitoring and Prediction*,  
681 65 (1): 450–59. <https://doi.org/10.1016/j.jmarsys.2006.01.017>. 2007.

682 Tappan, H., and A. R. Loeblich. « Foraminiferal evolution, diversification, and extinction ». *Journal of  
683 Paleontology* 62 (5): 695–714. 1988.

684 Wesslander, K., L. Andersson, P. Axe, J. Johansson, J. Linders, N. Nixelius, and A.-T. Skjervik. « SMHI  
685 Report: Swedish national report on eutrophication status in the Skagerrak, Kattegat and the  
686 Sound ». *Report Oceanography* No 54. 2016.

687 Yanko, V., A. J. Arnold, and W. C. Parker. « Effects of marine pollution on benthic foraminifera ». In  
688 *Modern Foraminifera*, 217–35. Springer Netherlands. [https://doi.org/10.1007/0-306-48104-9\\_13](https://doi.org/10.1007/0-306-48104-9_13).  
689 1999.

690

691

692 Figures

693 Figure 1. Map of the studied area. The star shows the focused station of this study. General water  
694 circulation: main surface currents (black arrows) and main deep currents (grey arrows). GB:  
695 Great Belt; LB: Little Belt; AW: Atlantic Water; CNSW: Central North Sea Water; JCW; Jutland  
696 Coastal Water; NCC: Norwegian Coastal Current; BW: Baltic Water. Insert source: [© BSHC](#).

697 Figure 2. CTD profiles of temperature, salinity, pH and dissolved oxygen concentration in the  
698 water column for the DV-1 station (modified from Charrieau et al. 2018).

699 Figure 3. Seasonal variability of salinity, temperature, pH and dissolved inorganic nitrogen  
700 (DIN) concentration at the surface water (light grey), and seasonal variability of salinity,  
701 temperature, pH and dissolved oxygen concentration at the bottom water (40–50 m) (dark grey)  
702 of the Öresund. The data were measured between 1965 and 2016 by the SMHI (Swedish



703 Meteorological and Hydrological Institute) at the station W LANDSKRONA. The number of  
704 measurements is indicated for each month.

705 Figure 4. Age-depth calibration for the sediment sequence from the Öresund (DV-1). A) Total  
706 and supported  $^{210}\text{Pb}$  activity. B) Unsupported  $^{210}\text{Pb}$  activity and the associated age-model. C)  
707  $^{137}\text{Cs}$  activity. The peak corresponds to the Chernobyl reactor accident in 1986. D) Age-depth  
708 model for the whole sediment sequence based on  $^{210}\text{Pb}$  dates and calculated sediment  
709 accumulation rates (SAR).

710 Figure 5. A) Relative abundances (%) of the foraminiferal major species (>5 %), benthic  
711 foraminiferal accumulation rate (BFAR, specimens.cm $^{-2}.\text{yr}^{-1}$ ), Shannon index, organic linings  
712 (specimens.cm $^{-2}.\text{yr}^{-1}$ ) and factors from the correspondence analysis. B) Benthic foraminiferal  
713 accumulation rates (specimens.cm $^{-2}.\text{yr}^{-1}$ ) of the major species (>5%), BFAR (specimens.cm $^{-2}.\text{yr}^{-1}$ ),  
714 Shannon index, organic linings (specimens.cm $^{-2}.\text{yr}^{-1}$ ) and factors from the correspondence  
715 analysis. Foraminiferal zones based on cluster analysis. Note the different scale on the x axes.

716 Figure 6. Dendrogram produced by the cluster analysis based on the Morisita index and the  
717 UPGMA clustering method.

718 Figure 7. Sediment parameters of the cores DV-1I and DV-1G ( $^{210}\text{Pb}$  dated): total organic carbon  
719 content (C<sub>org</sub>) (%), C/N ratio, and grain size (%). Foraminiferal zones indicated.

720 Figure 8. South-North flow (VAV) in the Öresund (dark line) and West-East flow (UAV) in the  
721 Kattegat (light line) between 1950 and 2013. Foraminiferal zones indicated.

722 Figure 9. A) NAO index for boreal winter (December to March), data from Jones et al. (1997).  
723 B) Variations of near-surface (10 m) wind conditions (October to March), data from Schenk and



724 Zorita (2012). Both NAO index and wind speed data are normalized on the period 1850-2008  
725 and show running decadal means. C) BFAR, percentage of sand fraction and West-East flow  
726 (UAV) in the Kattegat. Foraminiferal zones indicated.

727 Plate 1. SEM pictures of the major foraminiferal species (>5%). 1. *Stainforthia fusiformis*; 2.  
728 *Nonionellina labradorica*; 3. *Nonionella* sp. T1; 4. *Nonionoides turgida*; 5. *Eggerelloides*  
729 *medius/scabrus*; 6. *Bulimina marginata*; 7. *Ammonia batava*; 8. *Reophax subfusiformis*; 9.  
730 *Elphidium magellanicum*; 10. *Elphidium clavatum*; 11-12. *Ammonia* sp.

731 Tables

732 Table 1. Significant foraminiferal species and scores according to the correspondence analysis.  
733 Table 2. Ecological significance of the benthic foraminiferal assemblages (major species).

734 Appendix

735 Appendix A. Time series of salinity, temperature and dissolved oxygen concentration at the  
736 bottom water (40 m) of the Öresund between 1986 and 2013. The data were measured by the  
737 SMHI (Swedish Meteorological and Hydrological Institute) at the station W LANDSKRONA.

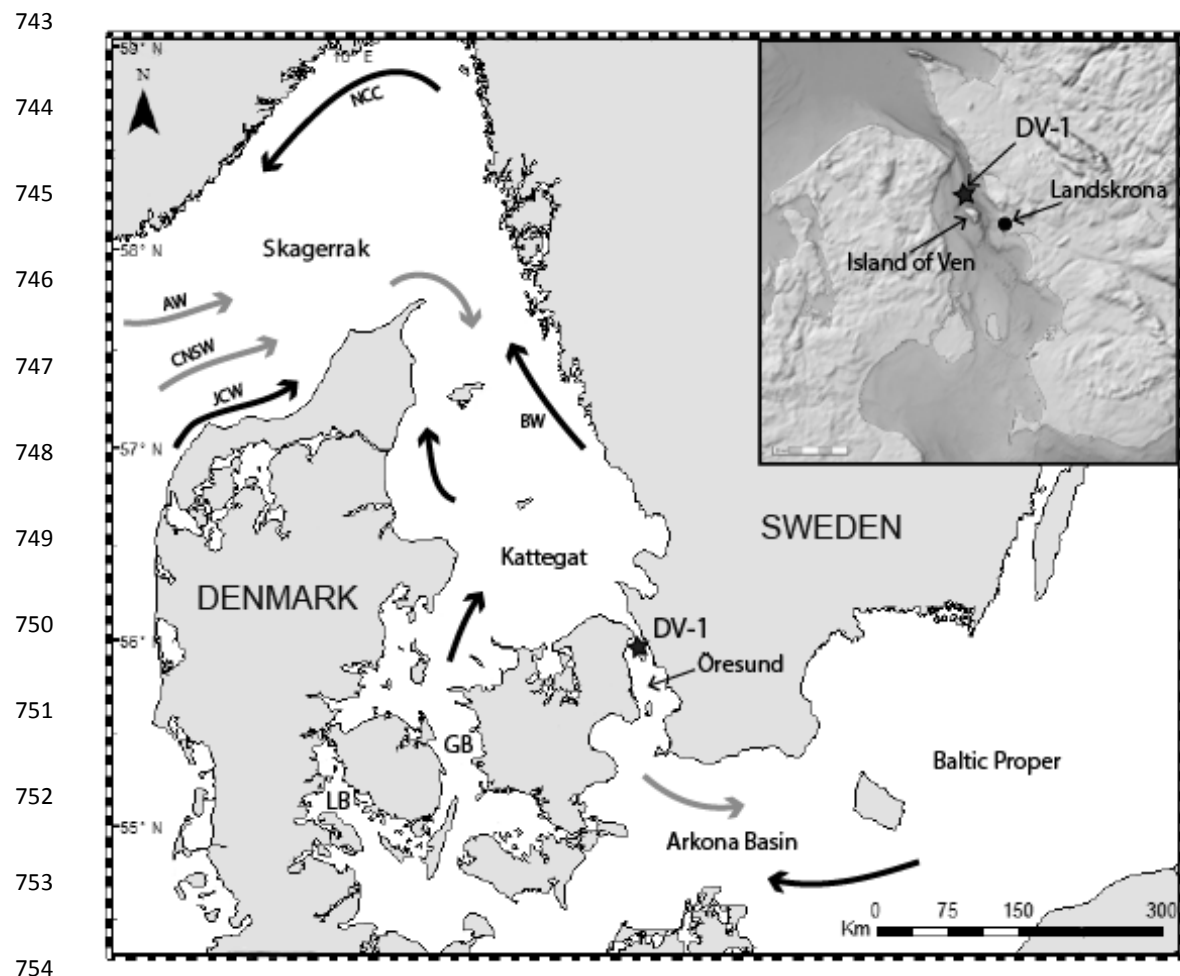
738 Appendix B. Total faunas, normalized to 50 cm<sup>3</sup>

739

740

741

742



755 Figure 1. Map of the studied area. The star shows the focused station of this study. General water  
756 circulation: main surface currents (black arrows) and main deep currents (grey arrows). GB:  
757 Great Belt; LB: Little Belt; AW: Atlantic Water; CNSW: Central North Sea Water; JCW; Jutland  
758 Coastal Water; NCC: Norwegian Coastal Current; BW: Baltic Water. Insert source: [© BSHC](#).

759

760

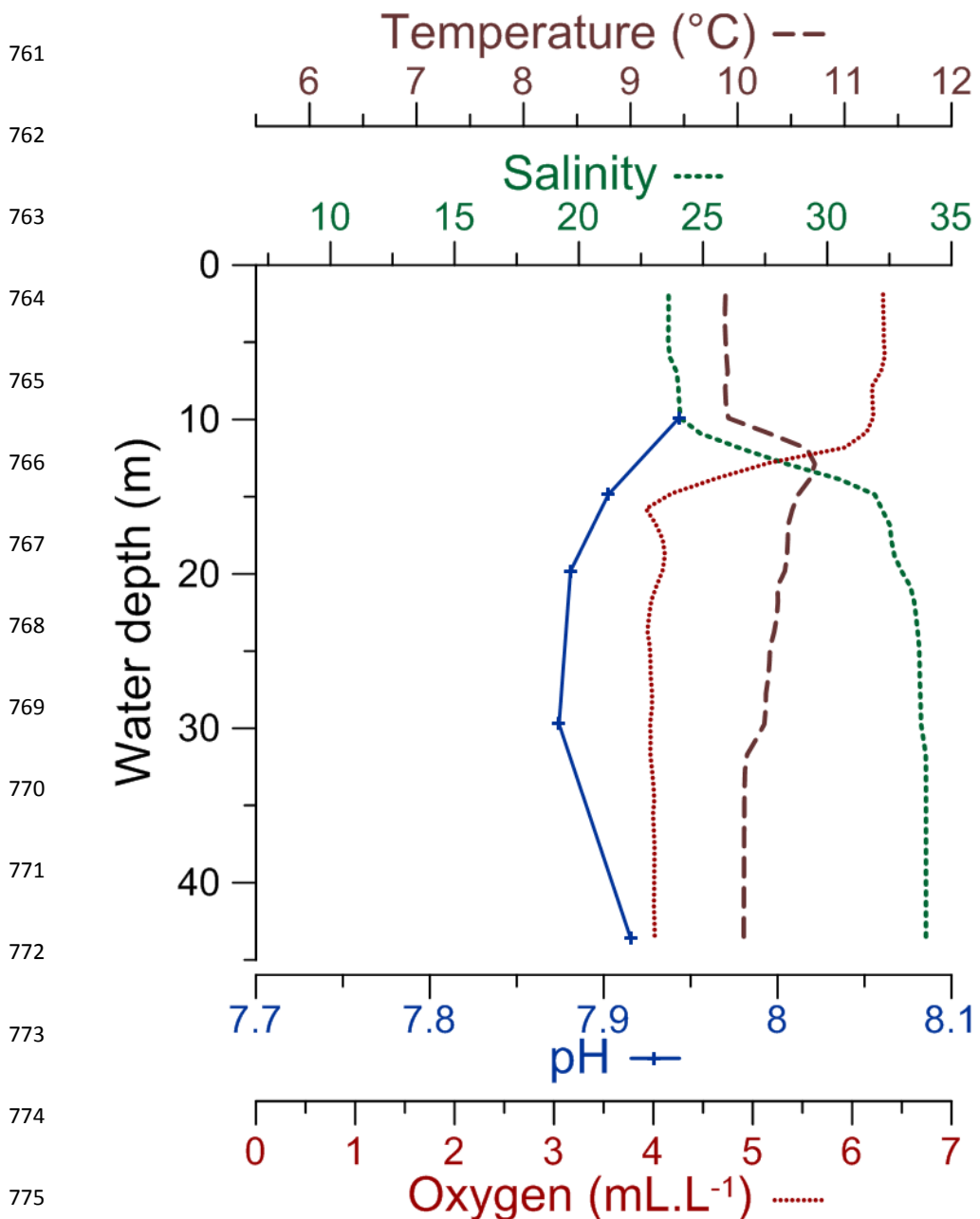
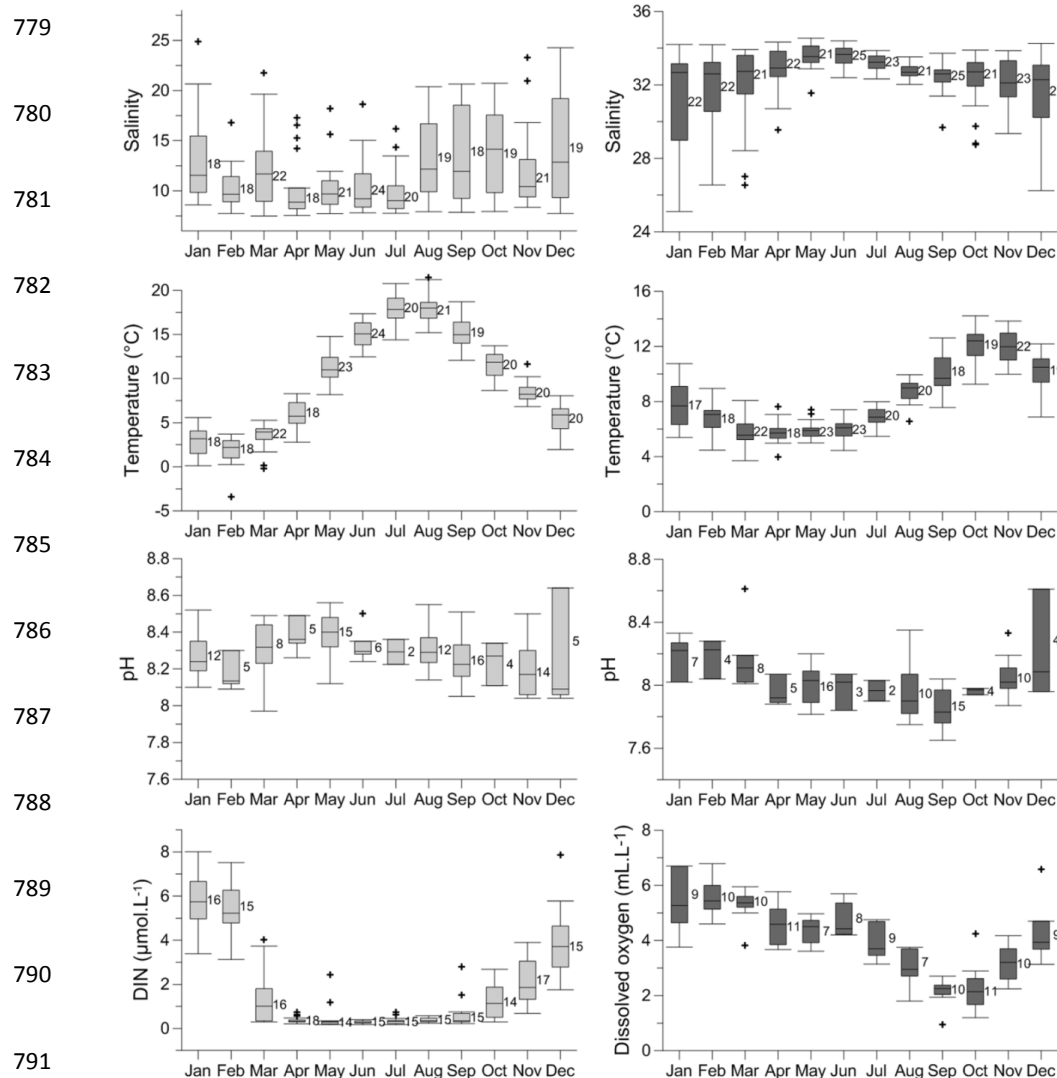
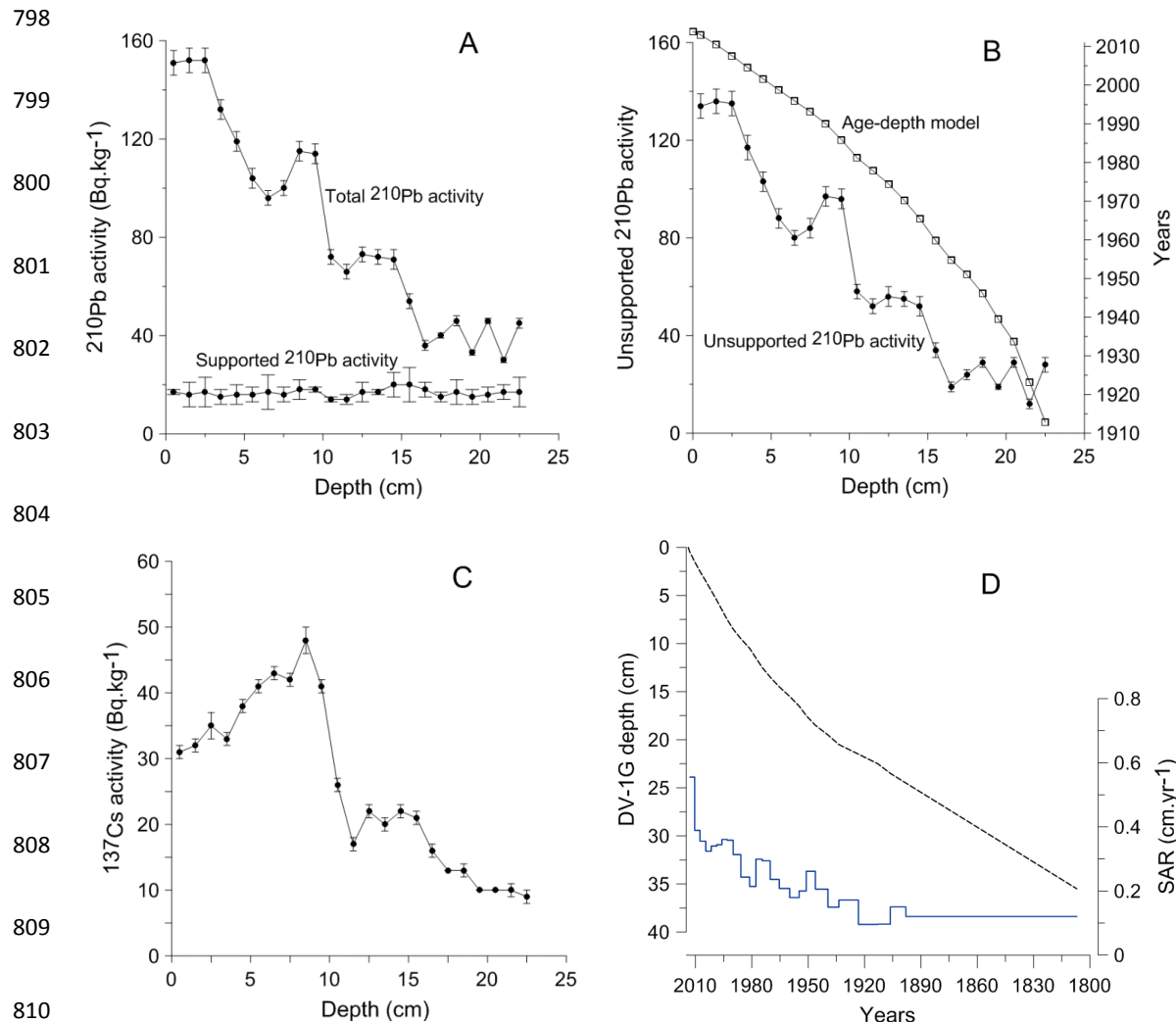


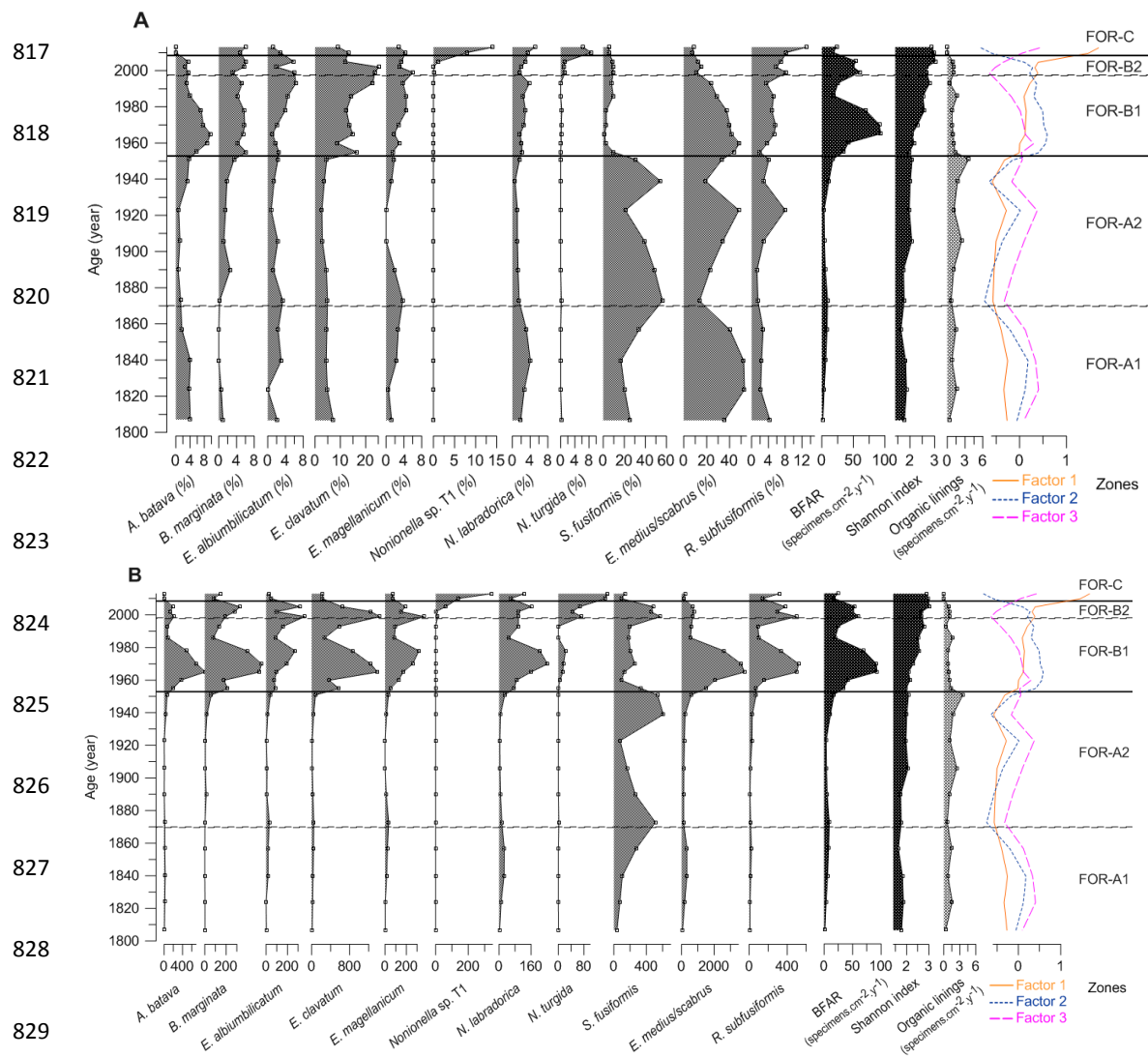
Figure 2. CTD profiles of temperature, salinity, pH and dissolved oxygen concentration in the water column for the DV-1 station (modified from Charrieau et al. 2018).



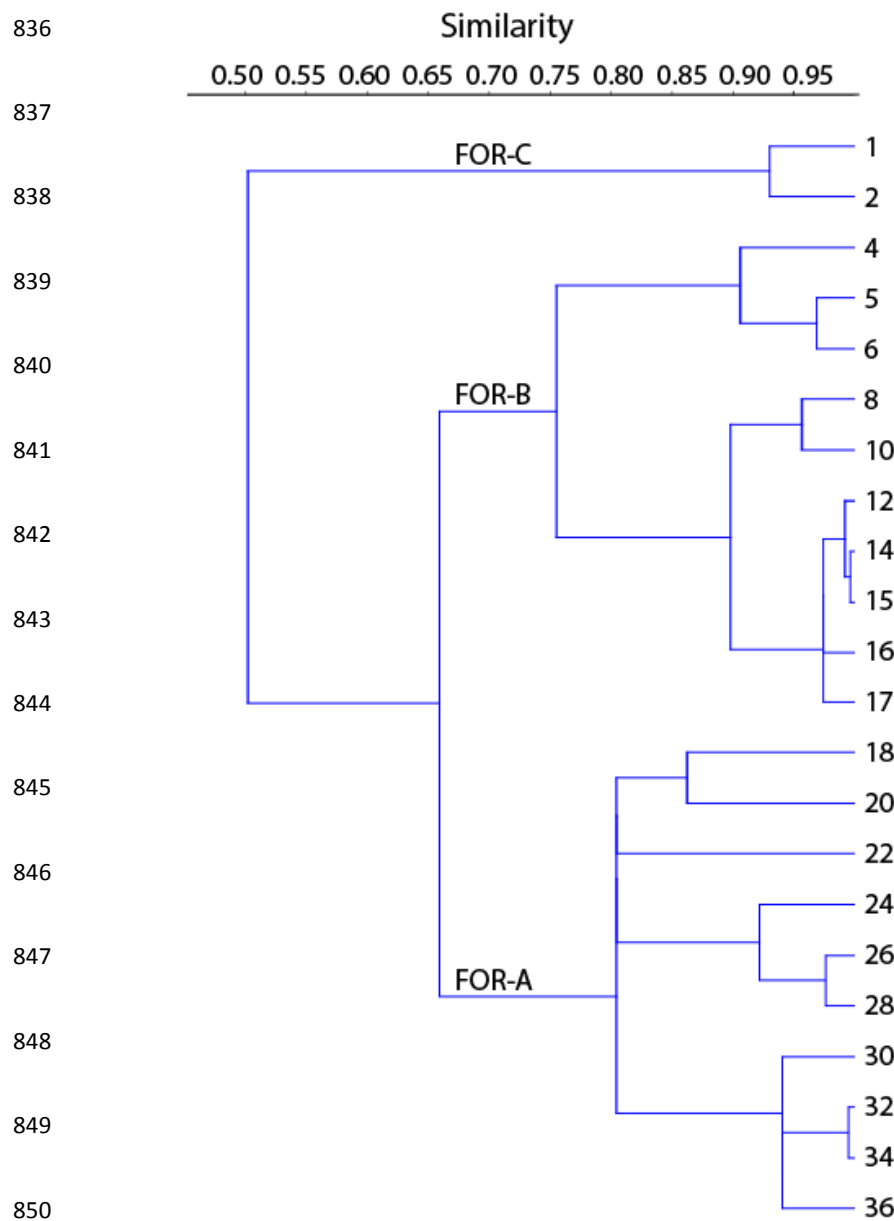
792 Figure 3. Seasonal variability of salinity, temperature, pH and dissolved inorganic nitrogen  
793 (DIN) concentration at the surface water (light grey), and seasonal variability of salinity,  
794 temperature, pH and dissolved oxygen concentration at the bottom water (40-50 m) (dark grey)  
795 of the Öresund. The data were measured between 1965 and 2016 by the SMHI (Swedish  
796 Meteorological and Hydrological Institute) at the station W LANDSKRONA. The number of  
797 measurements is indicated for each month.



811 Figure 4. Age-depth calibration for the sediment sequence from the Öresund (DV-1). A) Total  
812 and supported  $^{210}\text{Pb}$  activity. B) Unsupported  $^{210}\text{Pb}$  activity and the associated age-model. C)  
813  $^{137}\text{Cs}$  activity. The peak corresponds to the Chernobyl reactor accident in 1986. D) Age-depth  
814 model for the whole sediment sequence based on  $^{210}\text{Pb}$  dates and calculated sediment  
815 accumulation rates (SAR).



830 Figure 5. A) Relative abundances (%) of the foraminiferal major species (>5 %), benthic  
831 foraminiferal accumulation rate (BFAR, specimens.cm<sup>-2</sup>.yr<sup>-1</sup>), Shannon index, organic linings  
832 (specimens.cm<sup>-2</sup>.yr<sup>-1</sup>) and factors from the correspondence analysis. B) Benthic foraminiferal  
833 accumulation rates (specimens.cm<sup>-2</sup>.yr<sup>-1</sup>) of the major species (>5%), BFAR (specimens.cm<sup>-2</sup>.yr<sup>-1</sup>)  
834 <sup>1</sup>), Shannon index, organic linings (specimens.cm<sup>-2</sup>.yr<sup>-1</sup>) and factors from the correspondence  
835 analysis. Foraminiferal zones based on cluster analysis. Note the different scale on the x axes.



851 Figure 6. Dendrogram produced by the cluster analysis based on the Morisita index and the  
852 UPGMA clustering method.

853

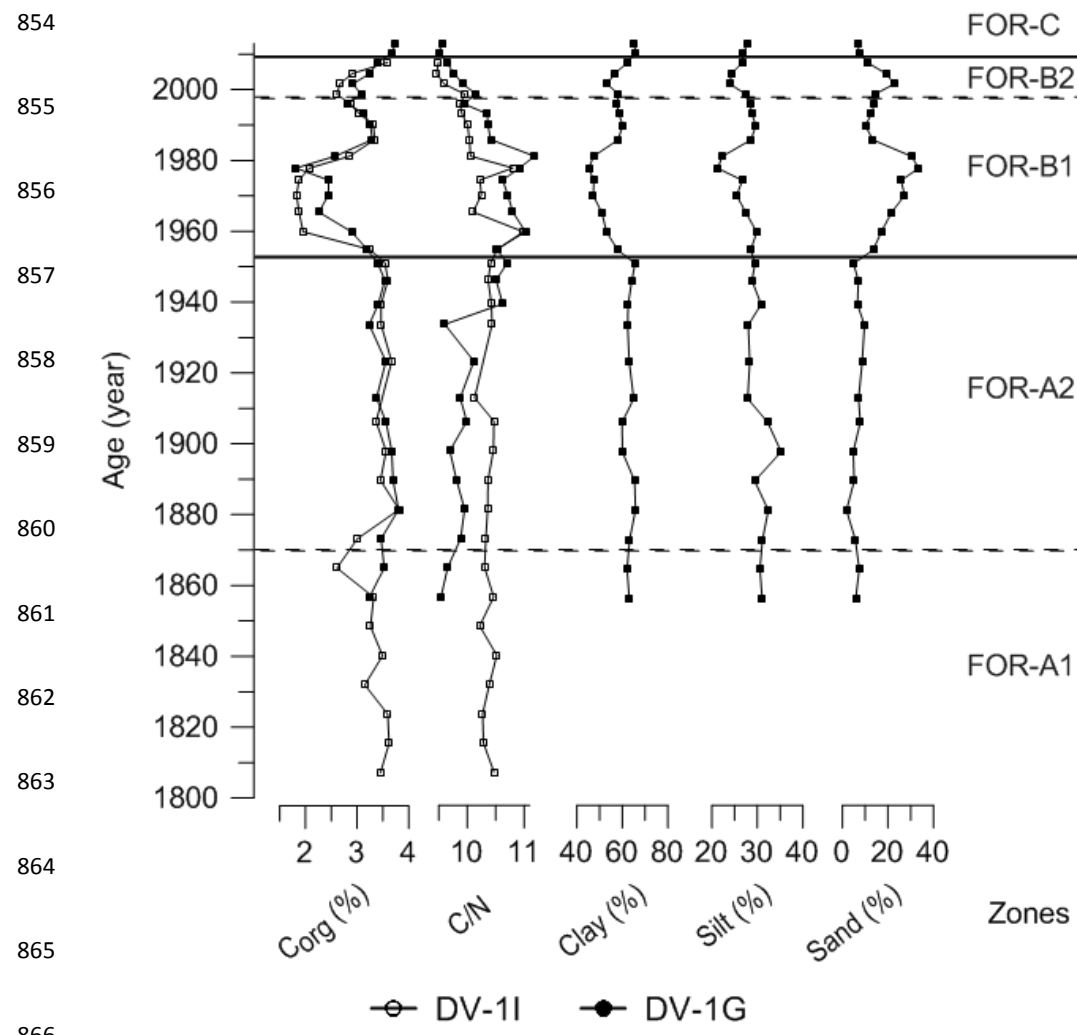
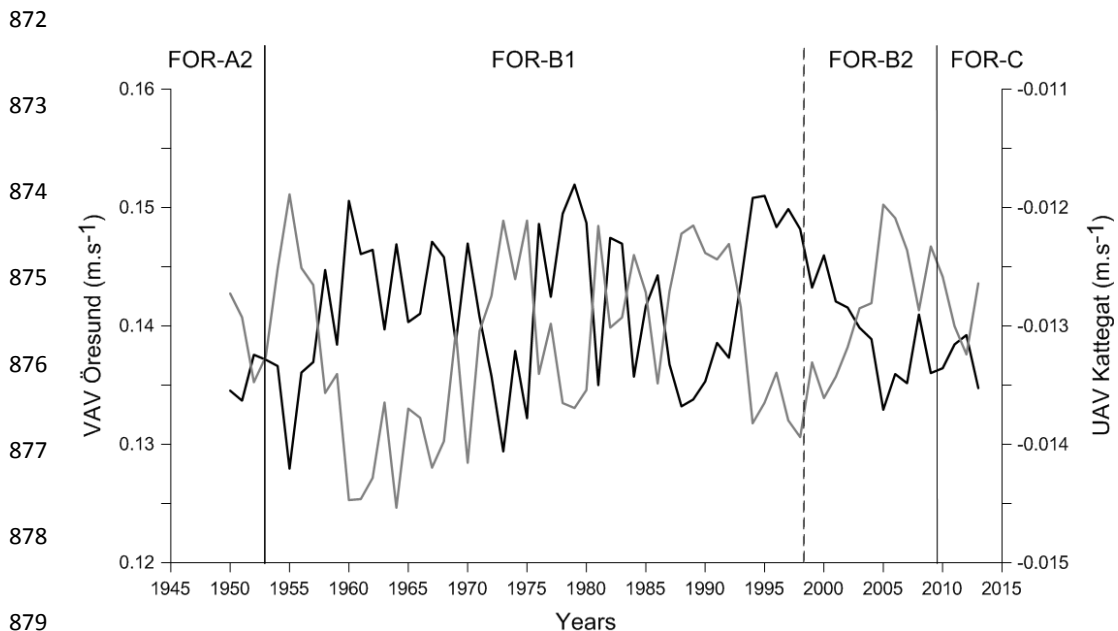


Figure 7. Sediment parameters of the cores DV-1I and DV-1G ( $^{210}\text{Pb}$  dated): total organic carbon content ( $\text{C}_{\text{org}}$ ) (%), C/N ratio, and grain size (%). Foraminiferal zones indicated.

869

870

871



880 Figure 8. South-North flow (VAV) in the Öresund (dark line) and West-East flow (UAV) in the  
881 Kattegat (light line) between 1950 and 2013. Foraminiferal zones indicated.

882

883

884

885

886

887

888

889

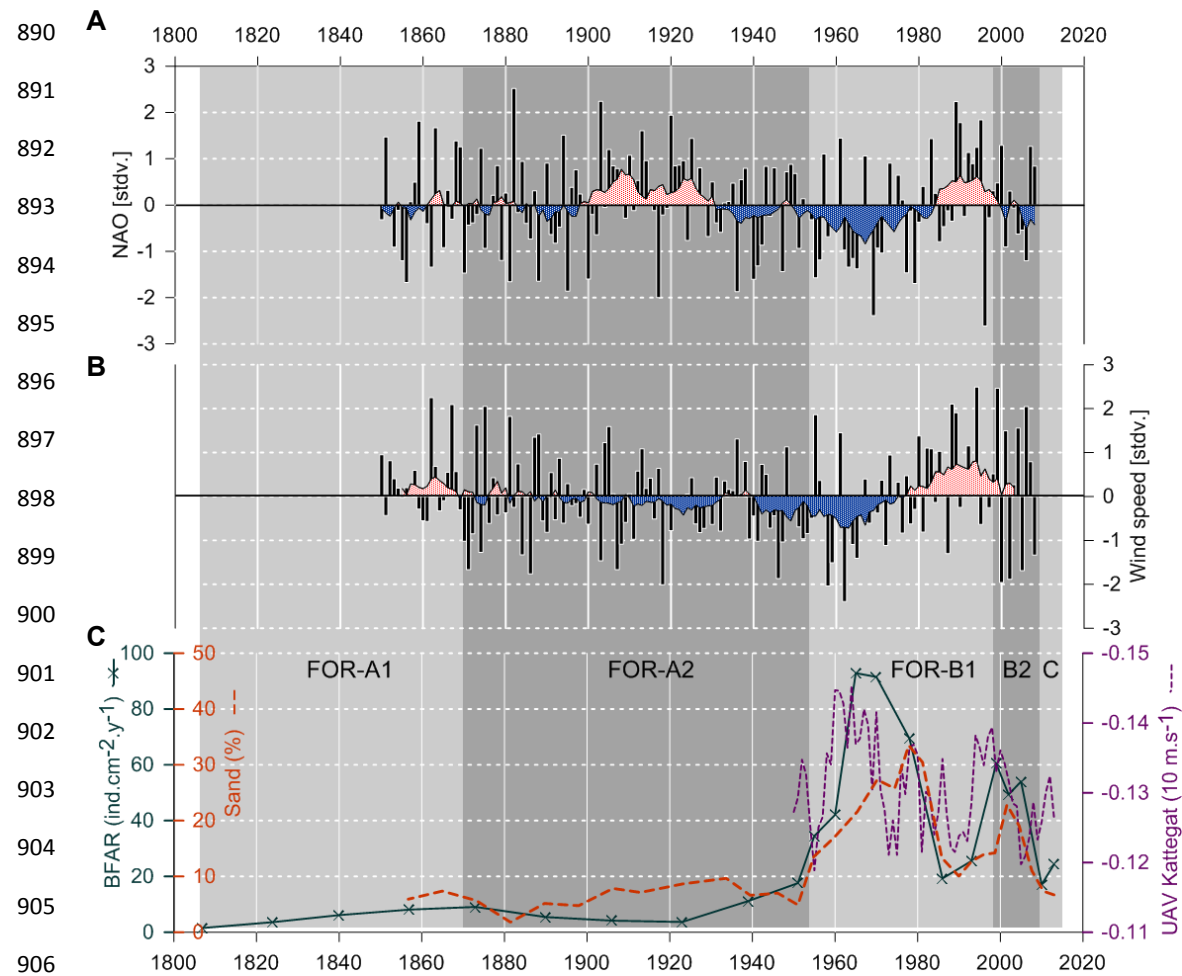


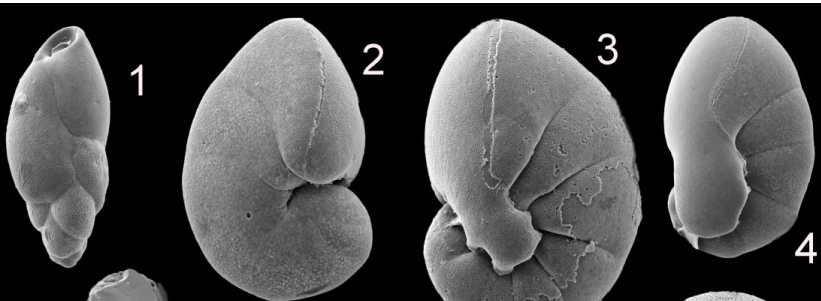
Figure 9. A) NAO index for boreal winter (December to March), data from Jones et al. (1997).  
B) Variations of near-surface (10 m) wind conditions (October to March), data from Schenk and Zorita (2012). Both NAO index and wind speed data are normalized on the period 1850-2008 and show running decadal means. C) BFAR, percentage of sand fraction and West-East flow (UAV) in the Kattegat. Foraminiferal zones indicated.

912

913



914



915

916

917

918

919

920

921

922

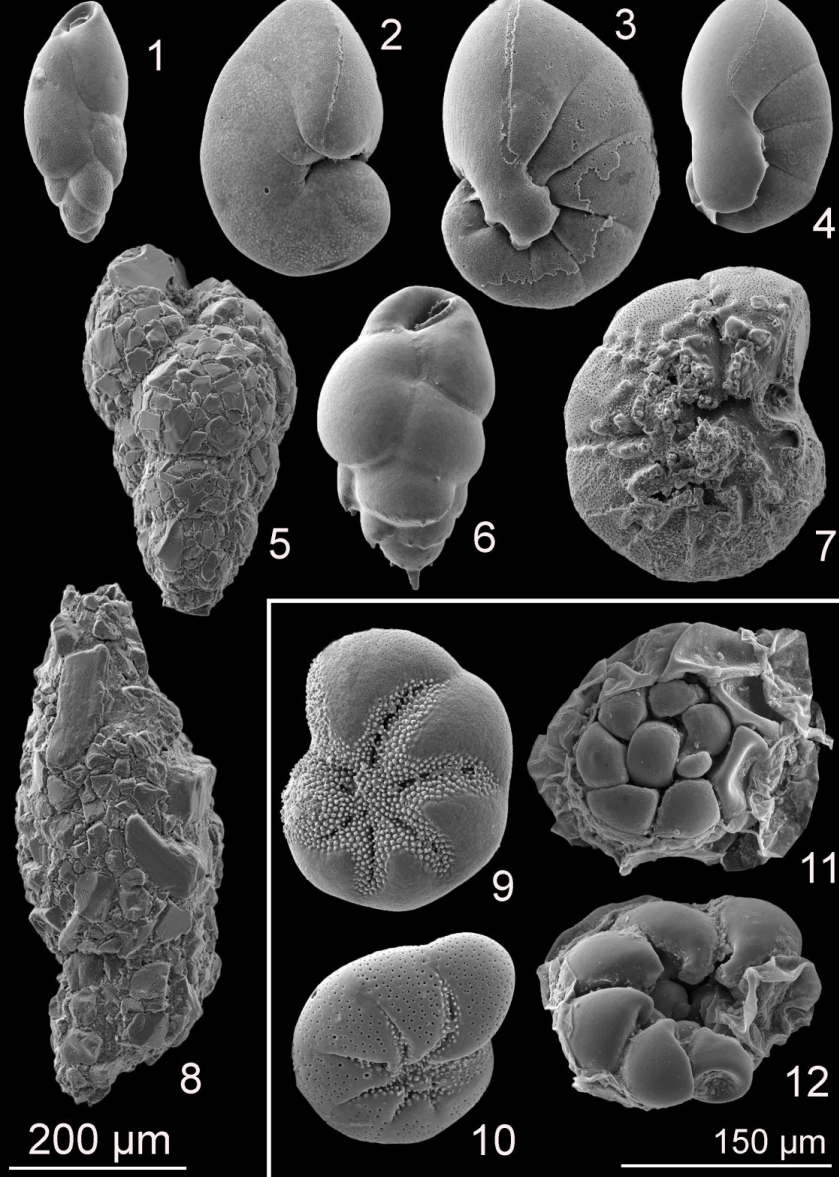
923

924

925

926

927



928 Plate 1. SEM pictures of the major foraminiferal species (>5%). 1. *Stainforthia fusiformis*; 2. 929 *Nonionellina labradorica*; 3. *Nonionella* sp. T1; 4. *Nonionoides turgida*; 5. *Eggerelloides* 930 *medius/scabrus*; 6. *Bulimina marginata*; 7. *Ammonia batava*; 8. *Reophax subfusiformis*; 9. 931 *Elphidium magellanicum*; 10. *Elphidium clavatum*; 11-12. *Ammonia* sp.



932 Table 1. Significant foraminiferal species and scores according to the correspondence analysis.

Factor	Total variance (%)	Significant species	Score
1	48.18	<i>Nonionella</i> sp. T1	5.10
		<i>Nonionoides turgida</i>	4.14
2	30.88	<i>Ammonia batava</i>	1.34
		<i>Stainforthia fusiformis</i>	-1.41
3	13.36	<i>Elphidium albiumbilicatum</i>	-1.65
		<i>Elphidium clavatum</i>	-1.57
		<i>Elphidium magellanicum</i>	-1.32

933

934

935

936

937

938

939

940

941

942

943

944

945

946



947 Table 2. Ecological significance of the benthic foraminiferal assemblages (major species).

Species	Ecological significance	Reference
<i>Ammonia batava</i>	Salinity 15-35, T 0-29°C, high tolerance to varying substrate and TOC	Alve and Murray (1999); Murray (2006)
<i>Bulimina marginata</i>	Tolerates low oxygen conditions, salinity 30-35, T 5-13°C, muddy sand, prefers organic rich substrates	Conradsen (1993); Murray (2006)
<i>Elphidium albiumbilicatum</i>	Salinity 16-26, typical brackish species	Alve and Murray (1999)
<i>Elphidium clavatum</i>	Tolerates low oxygen conditions, salinity 10-35, T 0-7°C, high tolerance to varying substrate and TOC, subtidal	Conradsen {Citation}; Alve and Murray (1999); Murray (2006)
<i>Elphidium magellanicum</i>	Coastal species	Sen Gupta (1999)
<i>Nonionella stella/aff. stella</i>	Tolerates low oxygen conditions, kleptoplastid, able of denitrification, invasive in the Skagerrak-Kattegat	Piña-Ochoa et al. (2010); Bernhard et al. (2012); Charrieau et al. (2018)
<i>Nonionellina labradorica</i>	Salinity >30, T 4-14°C, high latitudes, kleptoplastid, able of denitrification	Cedhagen (1991)
<i>Nonionoides turgida</i>	Opportunistic species, tolerates low oxygen conditions, prefers high food availability	Van der Zwaan and Jorissen (1991)
<i>Stainforthia fusiformis</i>	Opportunistic species, tolerates very low oxygen conditions, salinity >30, able of denitrification, prefers organic rich substrates, fast reproduction cycle	Alve (1994); Filipsson and Nordberg (2004); Piña-Ochoa et al. (2010)
<i>Eggerelloides medius/scabrus</i>	High tolerance to hypoxia, salinity 20-35, T 8-14°C, sandy-muddy sand, tolerance to various kind of pollution	Alve and Murray (1999); Alve (1990); Murray (2006); Cesbron et al. (2016)
<i>Reophax subfusiformis</i>	Tolerance to environmental variations	Sen Gupta (1999)

948

949

950

951

952

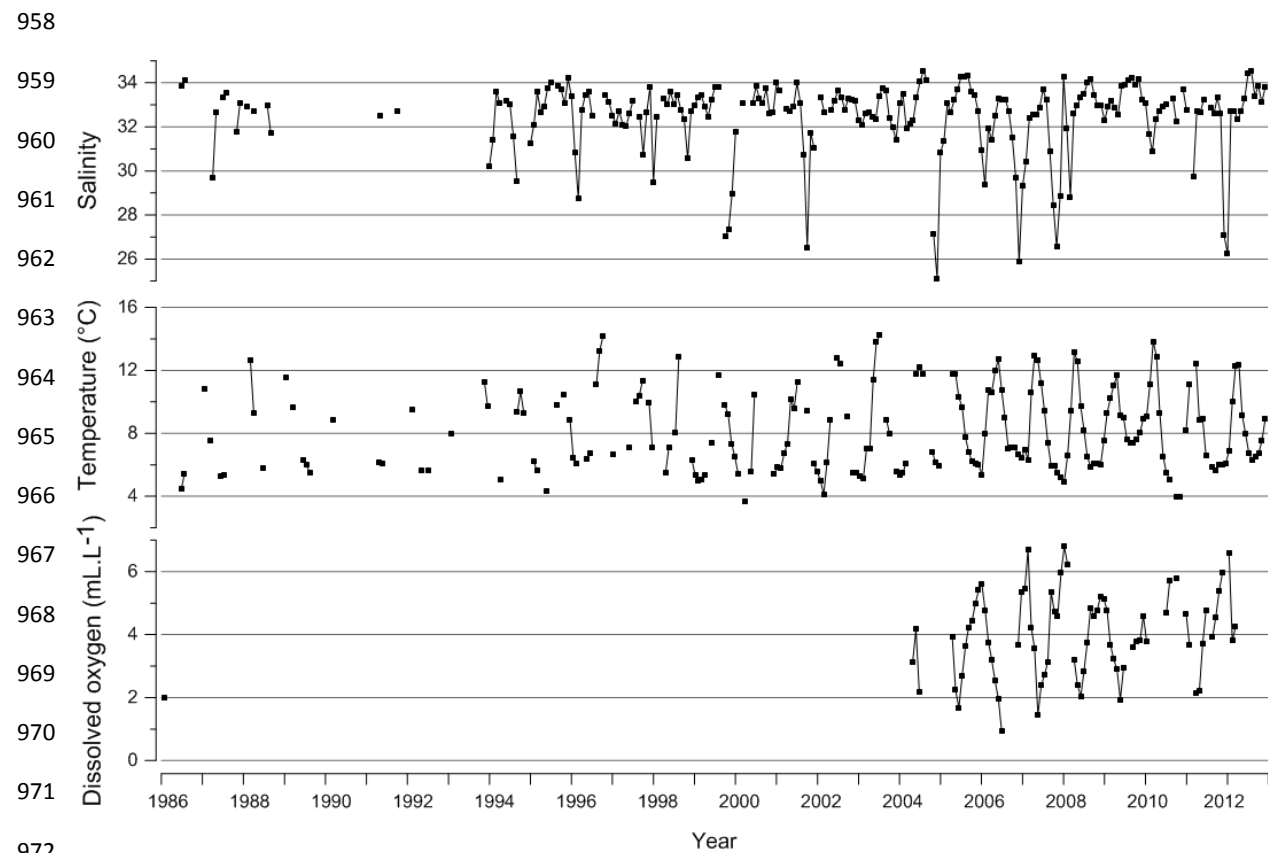
953

954

955

956

957



973 Appendix A. Time series of salinity, temperature and dissolved oxygen concentration at the  
974 bottom water (40 m) of the Öresund between 1986 and 2013. The data were measured by the  
975 SMHI (Swedish Meteorological and Hydrological Institute) at the station W LANDSKRONA.

976

977

978

979

980



Appendix B. Total faunas, normalized to 50 cm<sup>3</sup>

Station name FOR zones Centimeter Species	DV																FOR-A2						FOR-A1			
	FOR-C		FOR-B2			FOR-B1						FOR-A2				FOR-A1				FOR-A1						
	1	2	4	5	6	8	10	12	14	15	16	17	18	20	22	24	26	28	30	32	34	36				
<i>Biloculinella inflata</i>	6	13	0	0	0	0	0	0	0	0	0	0	0	0	0	0	0	0	0	0	0	0	0	0	0	0
<i>Cornuspira involvens</i>	0	6	9	0	0	0	0	0	0	0	0	0	0	0	0	0	0	0	0	0	0	7	0	0	0	0
<i>Pyrgo williamsoni</i>	1	1	0	16	0	0	0	0	0	0	0	0	0	0	0	0	0	0	0	0	0	28	0	0	0	0
<i>Quinqueloculina seminula</i>	0	1	0	0	35	0	14	0	0	0	0	30	0	0	0	0	0	0	0	0	0	0	0	0	0	0
<i>Quinqueloculina stalkeri</i>	6	0	9	0	18	0	0	0	0	0	0	0	0	0	0	0	0	0	0	7	14	0	0	0	0	0
<i>Porcelaneous varia</i>	13	31	111	32	0	0	0	0	34	8	46	0	0	8	0	0	0	0	0	7	9	0	0	0	0	0
Organic linings	0	0	146	159	158	60	345	132	171	238	304	332	686	575	599	807	444	260	608	316	649	159	0	0	0	0
<i>Ammonia beccarii</i>	0	0	292	191	308	105	159	822	1495	2167	1033	498	123	121	15	16	14	49	57	103	56	25	0	0	0	0
<i>Ammonia fallobeccharii</i>	57	77	69	80	35	37	111	350	854	986	516	231	85	23	15	0	0	0	0	0	0	0	0	0	0	0
<i>Ammonia</i> spp.	0	0	0	0	0	142	0	0	0	0	0	0	0	0	0	0	0	0	0	0	0	0	0	0	0	0
<i>Bolivina pseudoplicata</i>	0	0	9	0	0	0	0	0	0	68	0	0	0	0	0	0	0	0	0	0	0	0	0	0	0	2
<i>Bolivina pseudopunctata</i>	19	0	0	0	0	0	0	0	0	0	0	0	0	0	0	0	0	0	0	0	0	0	0	0	0	0
<i>Bolivina</i> spp.	0	0	9	0	0	0	0	19	0	0	0	0	0	0	0	0	0	0	0	0	0	0	0	0	0	0
<i>Buliminella marginata</i>	132	107	506	414	282	187	166	661	1128	1224	501	534	116	68	29	16	57	7	0	0	8	6	0	0	0	0
<i>Buliminella elegantissima</i>	0	6	206	143	176	60	83	57	103	170	61	29	8	8	7	8	0	70	7	9	0	0	0	0	0	0
<i>Cassidulina laevigata</i>	44	101	300	112	35	22	0	340	376	510	228	116	15	8	7	0	0	0	0	0	0	0	0	0	0	2
<i>Cassidulina reniforme</i>	0	13	17	32	0	15	14	19	68	0	15	14	0	0	0	0	0	0	0	0	0	0	0	0	0	0
<i>Cibicides lobatulus</i>	63	57	352	287	211	22	41	359	410	238	273	130	8	8	0	16	0	7	14	43	8	8	0	0	0	0
<i>Elphidium albiumbilicatum</i>	25	63	489	143	528	225	180	454	410	238	213	217	77	53	15	31	29	127	78	77	0	14	0	0	0	0
<i>Elphidium clavatum</i>	201	289	986	1833	2077	809	567	1436	2631	3331	1018	1430	154	136	51	39	100	183	155	111	72	45	0	0	0	0
<i>Elphidium magellanicum</i>	63	94	292	223	528	135	180	529	547	408	349	130	62	45	0	0	43	141	92	60	8	8	0	0	0	0
<i>Elphidium williamsoni</i>	19	19	86	32	18	22	14	113	68	136	61	14	0	0	0	0	7	28	21	51	16	6	0	0	0	0
<i>Elphidium</i> spp.	69	126	86	0	53	0	28	0	0	0	0	0	0	15	0	0	21	7	14	17	8	2	0	0	0	0
<i>Epistominella vitrea</i>	19	13	309	367	299	120	166	227	103	204	30	43	23	0	7	0	7	0	0	0	0	0	0	0	0	0
<i>Fissurina</i> spp.	0	0	0	0	0	0	0	0	34	0	15	0	0	0	0	0	0	0	0	0	0	0	0	0	0	0
<i>Parafissurina</i> spp.	0	0	43	16	35	22	0	38	34	68	15	14	8	0	0	0	0	7	0	0	0	0	0	0	0	0
<i>Furstenkoïna</i> spp.	0	0	0	0	0	0	0	0	0	0	0	0	0	0	0	0	0	7	0	0	0	0	0	0	0	0
<i>Gavelinopsis praegeri</i>	0	6	0	0	0	0	0	0	0	0	15	0	0	0	0	0	0	0	0	0	0	0	0	0	0	0
<i>Girodina</i> sp.	0	0	0	0	0	0	0	0	34	0	0	0	0	0	0	0	0	0	0	0	0	0	0	0	0	0
<i>Haynesina depressula</i>	25	25	51	0	0	0	0	0	0	0	0	0	0	0	0	0	0	0	0	0	0	0	17	0	0	0
<i>Hyalinea balthica</i>	0	19	9	0	0	7	0	0	34	0	0	0	0	0	0	0	0	0	0	0	0	0	0	0	0	0
<i>Lagena laevis</i>	0	0	0	0	0	7	0	0	0	0	15	0	0	0	7	0	7	14	0	0	0	0	0	0	0	0



Appendix B. Total faunas, normalized to 50 cm<sup>3</sup>

<i>Lagena semistriata</i>	0	0	0	0	18	0	0	0	0	0	0	0	0	0	0	0	0	0	0	0	0	0	0	0
<i>Lagena substriata</i>	0	13	9	32	53	22	14	0	34	34	0	0	15	15	0	8	14	14	0	9	0	0	0	0
<i>Lagena sulcata</i>	0	0	9	0	18	0	0	0	103	34	0	0	8	0	0	0	0	0	0	9	0	0	0	0
<i>Lenticulina</i> sp.	0	0	0	48	0	7	0	0	0	34	0	0	0	0	0	0	7	0	0	0	9	8	0	0
<i>Loxostomum</i> sp.	0	0	9	0	0	0	0	0	57	0	0	0	0	0	0	0	0	0	0	0	0	0	0	2
<i>Nonionella</i> sp. T1	308	176	94	0	18	0	0	0	0	0	0	0	0	0	0	0	0	0	0	0	0	0	0	0
<i>Nonionella</i> iridea	0	0	0	16	18	22	0	38	0	0	0	0	0	0	0	0	0	0	0	0	21	0	0	0
<i>Nonionellina</i> labradorica	113	75	249	143	141	135	97	340	513	382	243	188	54	23	22	16	29	56	106	103	40	12	0	0
<i>Nonionoides</i> turgida	138	189	103	64	106	0	0	38	34	34	15	0	0	0	0	0	0	7	0	0	0	0	2	0
<i>Nonionella</i> spp.	0	0	0	16	35	0	0	19	0	0	0	0	8	0	0	0	0	7	0	0	0	0	0	0
<i>Nonionellina</i> spp.	0	0	17	0	0	0	0	19	34	0	0	0	0	0	0	0	0	0	0	0	0	0	0	2
<i>Oolina</i> melo	6	0	0	0	0	0	0	19	0	68	0	0	0	0	0	0	0	0	0	0	0	0	0	0
<i>Polymorphina</i> spp.	0	0	9	16	0	0	0	38	0	0	15	0	0	15	0	0	7	0	7	9	0	0	0	0
<i>Procerolagena</i> clavata	0	6	0	0	0	0	0	0	0	0	0	0	0	0	0	0	0	0	0	0	0	0	0	0
<i>Procerolagena</i> grassilima	0	0	43	0	18	15	0	0	0	0	30	14	8	23	7	0	0	0	0	0	9	0	0	0
<i>Procerolagena</i> mollis	0	0	17	0	0	0	0	0	0	0	0	0	8	8	0	0	0	0	0	7	0	0	0	0
<i>Robertina</i> arctica	0	6	0	0	0	0	0	0	0	0	0	0	0	0	0	0	0	0	0	0	0	0	0	0
<i>Rosalina</i> spp.	0	0	0	32	0	0	0	0	0	102	0	0	0	0	0	0	0	0	0	0	0	0	0	0
<i>Stainforthia</i> fusiformis	126	119	746	669	827	277	373	340	547	306	258	838	1025	2029	402	541	1096	2112	1144	427	304	161	0	0
<i>Stainforthia</i> loeblichii	0	0	17	16	0	0	0	0	0	0	0	0	8	0	0	8	7	0	7	0	16	0	0	0
Hyalin indet (round)	0	0	9	0	0	0	0	0	68	68	15	14	15	0	0	0	7	14	14	0	0	0	2	0
Hyalin indet (twisted)	0	0	17	0	18	0	0	38	0	34	30	0	8	0	0	0	0	0	0	0	0	0	0	0
Hyalin varia	6	0	0	0	0	0	0	0	0	34	0	0	0	0	0	0	0	0	0	0	0	0	0	2
<i>Adercotryma</i> glomerata	13	44	206	127	35	0	14	0	0	0	0	0	15	0	0	0	0	0	0	0	0	0	0	0
<i>Ammodiscus</i> sp.	0	0	9	32	18	0	0	0	0	0	0	0	0	0	0	0	0	0	0	0	0	0	0	2
<i>Ammoscalaria</i> pseudospiralis	6	0	51	8	53	22	41	189	589	484	319	65	8	8	15	0	0	0	14	9	0	0	0	
<i>Ammotium</i> cassis	1	0	0	80	18	0	0	0	0	0	0	0	0	0	0	0	0	0	0	0	0	0	0	0
<i>Cribrostomoides</i> crassimargo	0	0	17	16	106	30	28	0	0	0	0	0	0	0	0	0	0	0	14	0	9	0	2	
<i>Cribrostomoides</i> subglobosum	0	2	0	0	0	0	0	19	0	0	0	0	0	0	0	0	0	7	0	0	0	0	0	0
<i>Cribrostomoides</i> spp.	0	0	206	207	317	45	69	19	103	170	46	116	62	38	44	16	21	28	14	26	16	2	0	0
<i>Recurvooides</i> spp.	57	44	0	0	53	0	28	0	0	0	0	0	0	0	0	0	0	0	0	0	0	0	0	0
<i>Eggerelloides</i> medius/scabrus	189	170	1055	1115	986	847	1133	4327	7756	9279	5696	3769	1125	712	920	470	516	514	1349	1325	793	223	0	0
<i>Haplophragmoides</i> bradyi	6	0	0	0	0	0	0	0	0	0	0	0	0	0	0	0	0	0	0	0	0	0	0	0
<i>Lagenammina</i> difflugiformis	25	6	26	0	70	0	0	0	26	0	76	0	0	0	7	8	7	14	0	17	0	8	0	0
<i>Leptohalysis</i> scotti	63	25	0	0	0	0	0	0	0	0	0	0	0	0	0	0	0	0	0	0	0	0	0	0
<i>Miliammina</i> fusca	0	0	26	32	0	7	0	19	0	102	0	0	0	23	0	0	7	21	7	9	0	2	0	0



Appendix B. Total faunas, normalized to 50 cm<sup>3</sup>

	0	0	0	0	0	0	102	0	14	0	0	0	0	0	0	0	0	0	0	0	0	0	0
<i>Paratrochammina haynesi</i>	0	0	0	0	0	0	0	0	0	0	0	0	0	0	0	0	0	0	0	0	0	0	0
<i>Psammosphaera bowmanni</i>	6	0	0	0	18	0	14	0	0	0	0	0	0	0	0	0	0	0	0	0	0	0	0
<i>Reophax subfusiformis</i>	285	181	583	430	722	127	207	557	1102	1198	440	173	139	106	153	39	29	56	92	60	32	27	
<i>Reophax</i> spp.	0	0	0	0	0	0	14	0	0	0	0	0	0	0	0	0	0	0	0	0	0	0	0
<i>Spiroplectammina biformis</i>	19	50	343	207	282	30	138	0	0	0	0	0	0	62	83	22	47	43	42	35	0	0	20
<i>Textularia earlandi</i>	57	0	60	0	88	0	0	0	0	0	0	0	0	0	8	0	0	0	7	0	0	0	0
<i>Textularia kattegatensis</i>	0	6	0	0	0	0	0	0	0	0	0	0	0	0	0	0	0	0	0	0	0	0	0
<i>Textularia</i> spp.	0	0	26	0	0	7	0	0	0	0	0	0	0	0	0	0	0	0	0	0	0	0	0
<i>Rotaliammina adaperta</i>	0	0	0	32	53	22	41	0	34	68	46	14	8	23	15	0	29	21	21	9	8	12	
<i>Trochammina</i> spp.	0	0	0	0	53	0	28	19	0	102	46	29	8	0	0	24	0	21	0	9	0	0	
Agglutinated varia	6	19	137	0	0	0	0	76	0	0	0	0	100	114	139	78	136	77	92	0	104	31	
TOTAL	2192	2198	8472	7418	8933	3620	4304	11725	19544	22561	12015	8968	4045	4308	2511	2187	2694	4013	3963	2854	2147	788	